Solution Combustion Synthesis for Preparation of Structured Catalysts: A Mini-Review on Process Intensification for Energy Applications and Pollution Control[1]

S. Specchia[a, b, *], **G. Ercolino**[a], **S. Karimi**[c], **C. Italiano**[b], **and A. Vita**[b]

[a]*Department of Applied Science and Technology, Politecnico di Torino, Torino, 10129 Italy*
[b]*Consiglio Nazionale delle Ricerche, Istituto di Tecnologie Avanzate per l'Energia "Nicola Giordano", Messina, 98126 Italy*
[c]*School of Chemistry, College of Science, University of Tehran, Tehran, 1417466191 Iran*
*e-mail: stefania.specchia@polito.it

Abstract—Solution combustion synthesis (SCS) is a preparation technique that can be used to synthesize a variety of inorganic nanomaterials and structured catalysts. It is based on a self-propagating exothermic redox reaction between organic salts and a fuel mixed together in an aqueous solution, which results in the formation of nanocrystalline and highly pure solid nanomaterials. SCS can be considered as an attractive synthesis method for catalysts due to the simple nature of the synthetic route and short reaction times. The process is easily scaled up to any kind of application which makes it economically attractive. This mini-review provides a short overview on the synthesis of structured catalysts by SCS and their recent utilization for energy applications and pollution control.

INTRODUCTION

In the recent years, solution combustion synthesis (SCS), also known as self-propagating high-temperature synthesis (SHS), has attracted the interest of many scientists as an intriguing technique to prepare catalysts for many different applications in a simple and easy way. Proof of this can be found in numerous review articles ([1–30] among the most famous) that have been published from the end of the 1960's. Starting in 1967, Russian scientists Merzhanov, Skhiro, and Borovinskaya first described this technique for the preparation of ceramic and intermetallic compounds, via solid flame combustion [31, 32]. In October 2007, after 40 years from this discovery, a dedicated international conference was held in Russia, with the presence of Merzhanov [33], to celebrate the anniversary of this methodology. Since then, this method also found extensive practical applications at the industrial level.

SCS is considered to be attractive for catalysts preparation due to the simple nature of the synthetic route, short reaction times, and relatively low cost [18, 28, 34, 35]. Furthermore, the composition, homogeneity, morphology, and stoichiometry can be finely

tuned to obtain the desired products that are highly crystalline and pure. Moreover, SCS allows the preparation of not only of nanomaterials and nanopowders but also, structured catalysts which carry on a thin film of catalytic material. This material can be easily coated in situ over any kind of ceramic or metallic surface for many different applications [36–46].

Figure 1 shows an overview of different supports that are normally used to prepare structured catalysts, where both the geometry (different shapes and porosity: monoliths, foams, tissues, corrugated plates, etc.) and the nature of the support (different materials: cordierite, alumina, zirconia, carborundum, metal alloys such as FeCrAlloy®, etc.) can vary greatly. The process can be easily scaled up and industrialized, which makes it economically attractive [18, 28].

THEORETICAL BASIS OF SCS

SCS is based on a self-propagating, exothermic, redox reaction between organic salts mixed with a fuel in either an aqueous solution or solid state [1, 6]. The precursors are gently heated to start the ignition of the reaction. The combination of an organic fuel, an oxygen source (oxidizer) and heat (ignition mode) results in a self-propagating combustion reaction which can

---

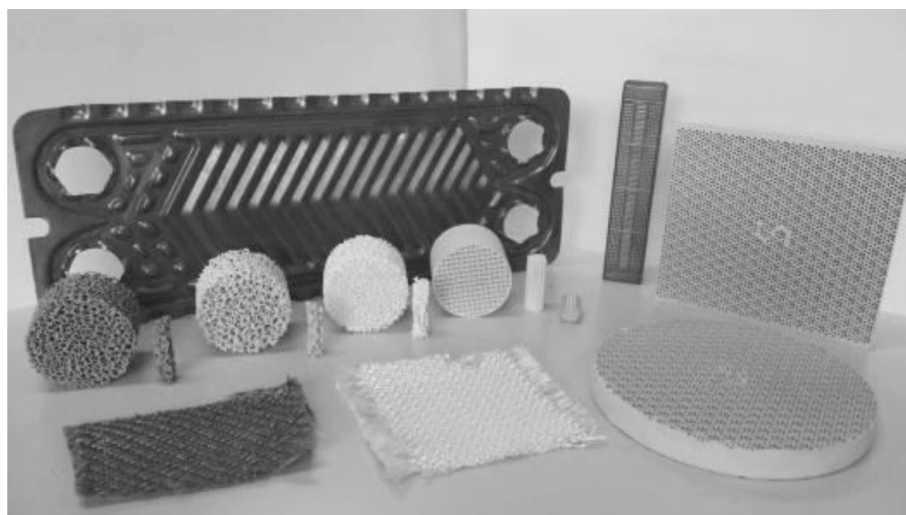[1] The article is published in the original.

Fig. 1. Examples of different ceramic and metallic supports that can be used to prepare structured catalysts by SCS (courtesy of Bekaert SA, Chauger Honeycomb Ceramics, Lanik s.r.o., Schwank GmbH, Worgas Bruciatori s.r.l.).
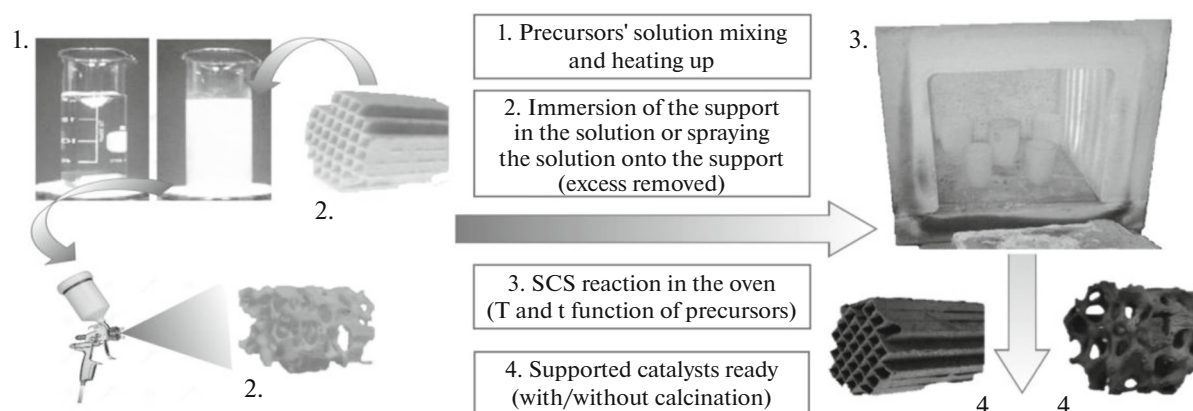

1. Precursors' solution mixing and heating up

2. Immersion of the support in the solution or spraying the solution onto the support (excess removed)

3. SCS reaction in the oven (T and t function of precursors)

4. Supported catalysts ready (with/without calcination)

Fig. 2. SCS used to prepare structured catalysts: in situ deposition of a thin layer of catalyst over monoliths and foams (by immersion or spraying).

be described using propellant chemistry [9, 47]. The intimate mixing, at a molecular level, of the precursors allows for uniform formation of the desired products. The initial combustion reaction self-propagates as a chemical reaction wave, starting with the reactive molecules which then involve the entire solution, via a front-layer heat transfer, to the final product. The reaction temperature, which reaches high values for a very short time, allows for the high degree of crystallinity and purity. Due to the combustion reaction, a large amount of gases are generated (mainly CO_2, H_2O, and N_2, with traces of CO and NO_x) within the short reaction time, favoring the formation of nano-sized powder with relatively high specific surface area. These gases inhibit crystallites growth and limit agglomerates, favoring the formation of a rather porous structure [28, 48, 49]. The synthesis is easily adaptable to any size of structured supports with any

shape and many starting materials for preparation of structured catalysts, as briefly illustrated in Fig. 2. To deposit in situ the catalyst, immersion, deep-coating, or spray-coating can be used indifferently, depending on the best operative conditions according to the final application [16, 43, 44, 50–52].

Any kind of solution containing an organic fuel and a metal precursor can, in principle, be used for SCS. The first pre-industrial preparation can be considered the one reached by Kingsley and Patil in 1998 [6]. They placed a mixture of aluminum nitrate and urea, dissolved in distilled water, in a muffle furnace at 500°C. The mixture boiled, foamed, and ignited with an incandescent flame at a temperature of approximately 1350°C. They produced a fluffy, fine, highly crystallized, nanosized α-alumina in less than 5 min, with a specific surface area of approximately 8 m^2 g^{-1}. Figure 3 shows the fine powder obtained by Kingsley

and Patil, together with the physicochemical characterization: the XRD spectrum is typical of α-alumina and the lattice constant parameters they calculated were in agreement with literature data [6]. SEM and TEM investigations enlightened the typical shape of the surface, characterized by a series of cracks and pores due to the formation of gases during the combustion reaction [6]. Despite the explosive nature of uncontrolled exothermic redox reactions, the combustion of the aluminum nitrate—urea mixtures is self-propagating and non-explosive [6, 7]. The advantage of the self-propagating combustion reaction lies in the large amount of gases that are generated within a short period of time.

Basically, SCS is a reaction of combustion between one or more metal nitrates (which acts as an oxidizer) and an organic fuel. Reagents can be mixed in an aqueous solution to favor intimate mixing at a molecular level, assuring a high degree of purity in the final product. Depending on the valence of the metal in the nitrate, the fuel-to-oxidizer ratio ϕ (the so-called elemental stoichiometric coefficient) represents the ratio between the total valences of the fuel and the total valences of the oxidizer. When ϕ is equal to 1, the reaction proceeds according to stoichiometric conditions and the initial mixture does not require atmospheric oxygen for completing the oxidation of fuel [18]. When $\phi > 1$ there are fuel-rich conditions (that is, oxygen is a product of the reaction), whereas when $\phi < 1$ this means there are fuel-lean conditions (that is, oxygen is a reagent of the reaction). Thus, a variation of ϕ means a variation of the amount of heat released during the reaction, and in turn a variation of the crystalline structure of the final product. In addition to this, ϕ also strongly influences the heat of reaction [47]. Numerous scientists have demonstrated that, for an ideal reaction (no heat losses), the heat of reaction becomes more exothermic while $\phi > 1$, whereas when $\phi \ll 1$ the reaction becomes endothermic [47, 23].

The low temperature decomposition of the organic fuel favors the ignition of the reaction. The ignition can be obtained either with a hot metal wire, or by placing the solution into an oven at a relatively low temperature, or into a microwave oven. This proceeds in a self-sustained fashion due to its exothermic and autocatalytic features [1, 28, 53]. Figure 4A shows a typical example of the effect of ϕ while synthesizing Co_3O_4 spinel by SCS (synthetic conditions: cobalt nitrate and urea as precursors, vigorously mixed in aqueous solution at different ϕ values, then placed in an oven for 20 min at 250°C [54]). While maintaining constant temperature of the oven, the ignition temperature of the reaction is anticipated and the maximum temperature recorded during self-propagation increases with ϕ. This is because of the increase of the exothermic level of the combustion reaction (appreciable by calculating the temperature of adiabatic flame, reported in Fig. 4b). The higher temperature
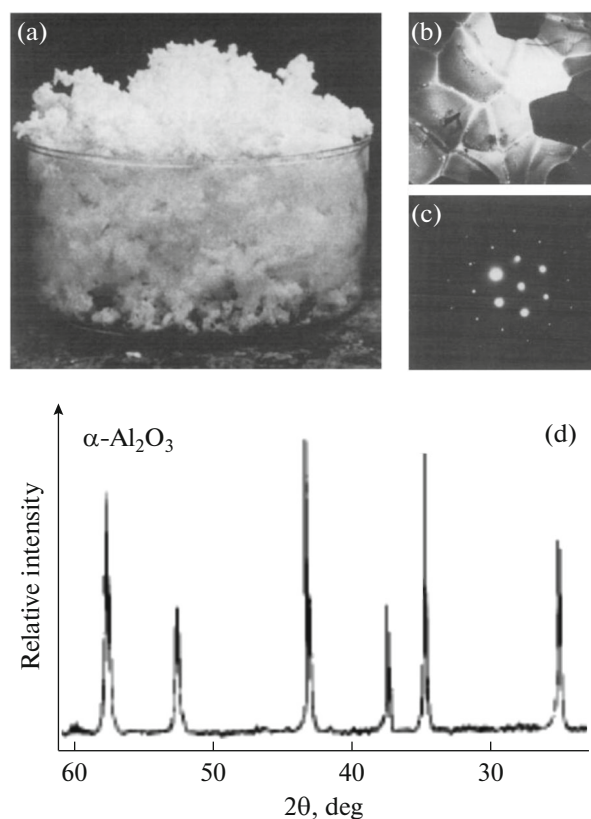

Fig. 3. α-Alumina synthesized by Kingsley and Patil in 1988: as-prepared foamy powder (a), TEM images (b, c), and XRD spectrum (d). Data rearranged from [6].

reached during the synthesis allows for a faster process and in turn, smaller average crystallite size. A variation of the ignition source temperature affects the whole SCS process. In particular, an increase of the temperature at which the reagents are exposed, boosts self-ignition by accelerating the reaction, thus allowing higher flame temperatures to easily be reached. Surely, the parameter which most affects the whole process is ϕ, which must be optimized case by case depending on the desired application of the final products.

The choice of the organic fuel plays another important role in the SCS process. Fuels fulfill various purposes: they help to homogeneously mix the organic precursors of the desired final products by favoring the formation of metal ion complexes [4, 9]. They decompose fast forming various compounds, aiding the combustion reaction, such as combustible gases HNO_3 and NH_3, which provide the necessary heat to complete the reaction [23, 49, 55]. The fuel allows for propellant chemistry, being a source of C and H atoms, it favors the formation of CO_2 and H_2O gaseous products which inhibit particle growth and form a porous structure [6, 7, 28, 48, 49]). Thus, fuels must possess at least the following properties: (*i*) being soluble in water and compatible with metal nitrates; (*ii*) having low ignition
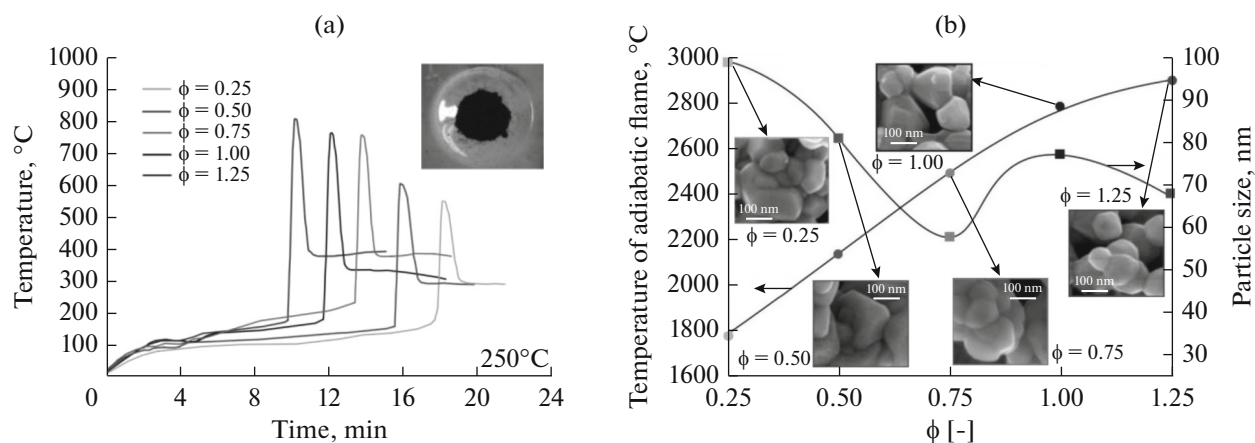
Fig. 4. Effect of the fuel-to-oxidizer ratio ϕ on the measured reaction temperature with the oven set at 250°C (a), adiabatic temperature of reaction (b), and crystallite dimensions during the synthesis of Co_3O_4 (b). Insets: FESEM images of Co_3O_4. Data partially rearranged from [53].

temperature (preferably below 500°C) and not explosive combustion reaction; (*iii*) developing a large amount of gases during combustion, possibly harmless; and (*iv*) being available, and preferably, cheap.

Simple compounds such as urea, glycine, alanine, glycerol, etc. are recognized as potential fuels [9, 55]. Compounds containing N−N bonds are well-known to better assist the combustion reaction, even if they act a drawback with the release of NO_x emissions during combustion [53]. In some cases, the use of highly viscous fuels, such as glycerol, helps obtain a better distribution of the final desired product on the structured catalyst support [53]. Table 1 lists the most common organic fuels typically employed in SCS, along with their main features.

Thus, SCS is a viable technique to produce useful materials such as advanced ceramics, catalysts, phosphors, pigments, composites, intermetallic, and nanomaterials [9, 18, 21−24, 28, 34, 35, 56−62].
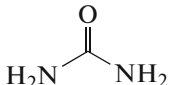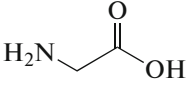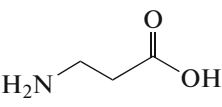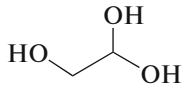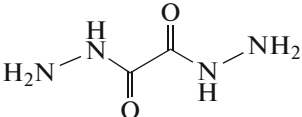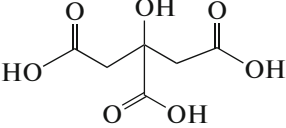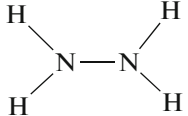
SCS FOR PROCESS INTENSIFICATION

Structured catalysts are widely used in energy-related and environmental applications, such as fuels production (syngas, hydrogen, biodiesel, etc.) [40−43, 64, 87, 96, 102−107], electrochemical processes and fuel cells [62, 95, 100, 108−116], stationary and automotive emission control systems [45, 46, 71, 77, 117−125], and catalytic redox processes [36, 37, 65, 72, 76, 126−130]. The preparation of highly active, well dispersed metal particles that are uniformly distributed over structured supports, plays a crucial role at an industrial level. SCS allows for the preparation of adhesive coatings on structures such as ceramic or metallic tissues, spheres, monoliths, foams, etc. Compared to other preparation techniques, SCS provides many advantages. The most common technique at an industrial level, the wash-coating, first requires a

detailed optimization of the various operative parameters, such as the concentration of the slurry, pH, viscosity, the speed of dipping, etc., to assure an adequate adhesive layer of catalyst on the surface of the structures [42, 52, 131, 132].

The World Energy Outlook 2016 [133], released by the International Energy Agency on November 2016, predicts a 30% increase of primary energy demand by 2040, due to growing population. To meet these needs, it is essential to respect the quality of air, water, and soil in order to take care of the environment and reduce local pollution, with regards to the recent Paris Agreement [134]. This agreement implies, on one hand, to increase energy production, on the other hand, to manage the continuous requirement of new products all while taking care of the environment. From this perspective, process intensification (PI) allows for a cleaner, safer, smaller, and more energy-efficient process design approach for any kind of technological application [135−137]. More specifically, SCS is seen as a manufacturing technique which allows for PI because of its intrinsic energy saving (low energy requirements only during the initial ignition step) [22, 30] and production of highly pure products. The high temperature, reached during the self-propagating exothermic reaction, does not require any additional energy source which allows for complete conversion of reactants into pure, high-quality products. In fact, any impurities present in the starting materials can easily volatilize during heating [22]. Moreover, SCS requires relatively cheap reactants, simple equipment, and low-cost facilities, leading to a reduction in production costs when compared to conventional manufacturing processes. Thus, SCS is an attractive, innovative, and intriguing technique to produce structured catalysts by PI [18, 20].

Precisely, structured catalysts based on monoliths and foams can provide many advantages with respect

Table 1. Fuels most commonly employed for SCS and some examples of synthesized products

Fuel	Structure	ΔH°_{comb}, kJ mol^{-1}	Synthesized products [refs]
Urea, CH_4N_2O		-633	Pt/CeO_2; Ni/CeO_2; Rh/Al_2O_3; Ni/Al_2O_3; Pd/Co_3O_4; CeO_2/ZrO_2; $Bi_xMo_yO_z$; $CaCu_3Ti_4O_{12}$; $LaCr_{0.9}O_3$ [41, 43, 63−71]
Glycine, $C_2H_5NO_2$		-974	Ni/CeO_2; Co_3O_4; Mn_3O_4; $LaMnO_3$; $La_{1-x}Sr_xM_xO_3$ (M = Fe, Co, Ni) [41, 67, 72−77]
β-Alanine, $C_3H_7NO_2$		-1329	Pt/CeO_2; $LaMO_3$ (M = Mn, Cr, Sr); $CoWO_4$; $La_{1-x}Sr_xM_xO_3$ (M = Fe, Co, Ni); $Ca_3Al_2O_6$; $CaAl_{12-2x}Ni_xTi_xO_{19}$ [72, 78−82]
Glycerol, $C_3H_8O_3$		-1654	$LaMnO_3$; $NiFe_2O_4$; $LiMn_2O_4$; $Co_3O_4/\gamma\text{-}Al_2O_3$; $CuCo_2O_4$; $CuCr_2O_4$ [53, 72, 83−86]
Oxalyl dihydrazide, $C_2H_6N_4O_2$		-1218	Pt/CeO_2; Ni/CeO_2; ZrO_2/CuO; CuO/CeO_2; [41, 74, 87−91]
Citric acid, $C_6H_8O_7$		-1961	$SrFeO_3$, $Sr_{0.85}Ce_{0.15}FeO_{3-x}$; Fe_2O_3; Fe_3O_4; Mn_2O_3 $Ni/Y_2O_3/ZrO_2$; Co/SiO_2; Al−Mn−Mg−O [61, 92−98]
Hydrazine, N_2H_4		-622	$BaTiO_3$; Fe_2O_3; Fe_3O_4; $MgCr_2O_4$; α-$CaCr_2O_4$; $La_{0.7}Ba_{0.3}MnO_3$; Fe_2O_3; Fe_3O_4 [9, 99−101]

to packed beds. In fact, they can operate at higher space velocity with reduced pressure drop due to their higher surface-to-volume ratio [138, 139]. Recently, open cell foams have been used as an attractive alternative for many different applications due to their high mechanical strength and enhanced heat transfer properties [140−142]. The characteristics of open cell foams as structured supports for catalysts, including their high porosity and tortuosity, provide better catalytic performance which allows for a reduced catalyst loading with good distribution on the surface of the structure, lower pressure drops, and enhanced heat transfer properties with high thermal stability [138, 139, 143−145]. These characteristics make these structured catalysts very attractive for highly exothermic or endothermic reactions (combustion or reforming processes), and also for low contact time reactions (partial oxidation processes) [138, 139, 143, 144]. Until now, very few publications are available in the literature on structured catalysts prepared by SCS : these few include articles that are most focused on the

preparation and characterization of the structured catalysts [53, 146], while others are more focused on the use of monoliths [37, 40, 42, 71, 77, 123, 126] or open cell foams [45, 46, 106] as structured catalysts for energy applications or pollution control.

SCS FOR PREPARATION OF STRUCTURED CATALYSTS BASED ON FOAMS

The preparation of highly dispersed metal particles uniformly covering structured supports plays a crucial role in many industrially important catalytic applications. This issue becomes important for three-way structured catalysts such as monoliths and foams. The metal deposition on the structures requires additional precursors to achieve a uniform distribution. In the literature, different approaches such as rotation of the impregnated monolith, freeze-drying, microwave heating, and spraying were proposed to improve the effectiveness of metal deposition on structured catalysts by SCS.
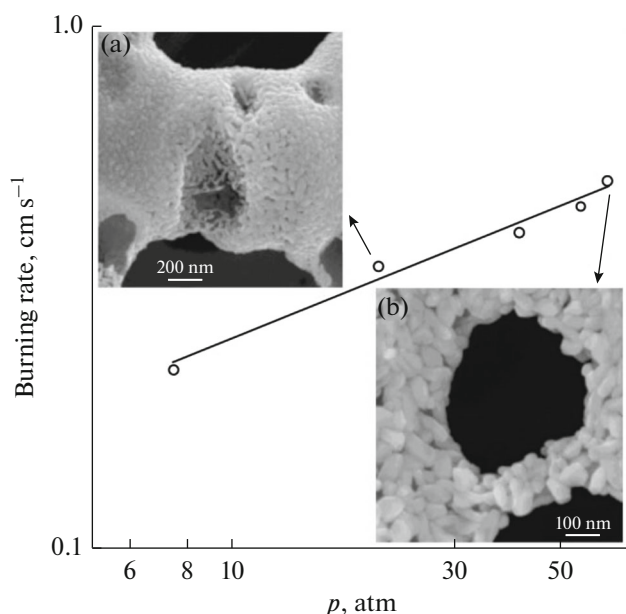
Fig. 5. Effect of pressure on the burning rate during the synthesis of Fe foams by SCS of Fe–bistetrazolamine complex. In the insets: SEM images of the grain size of Fe foams obtained at low (a) and high pressure (b). Data rearranged from [146].

Regarding the preparation of foams as structured supports, Tappan et al. synthesized ultra-low density nanostructured metal foams by SCS [146]. They prepared metal complexes based on Fe and bistetrazolamine, as the organic ligand, to form pellets. SCS was performed in an inert atmosphere to ignite the pellets, resulting in a vigorous burn producing sparks. In this case, the decomposition of the Fe–bistetrazolamine complex liberates gases, while Fe was reduced to an oxidation state of zero, giving rise to highly porous iron nanofoams. Varying the concentration of the Fe–bistetrazolamine complex, or the synthesis conditions (inert pressure, type of inert atmosphere, N_2 or Ar), allows for controlling the characteristics of the final nanostructured metal foams. Figure 5 shows the variation of the burning rate of Fe–bistetrazolamine complex, as a function of Ar pressure during SCS, together with the morphology obtained, enlightened via SEM. The structural size of Fe grains decreases at lower pressures, where their size was 30–50 nm attained at high pressure and 10–50 nm at low pressure. These authors demonstrated that it is possible to increase the specific surface area of these foams from 20 to 120 m^2 g^{-1}, after heat treatment at 500°C under hydrogen flow without altering the grain size. In fact, the heat treatment after SCS favors the removal of volatile elements while completing the densification process, considering the short time at which SCS occurs.

Zavyalova et al. [53] covered ceramic foams with a uniform film of Pt metal nanoparticles by microwave-assisted SCS. They dipped α-alumina foams into a solution of glycerol and Pt nitrate, pre-heated at 80°C for 2 h. After removing the excess of solution by spraying dry air, the dipped foams were placed into a microwave, set at 700 W, at a varied synthesis time of 3 to 9 min. Microwave irradiation provides rapid and selective heating of the precursors' solution. They adjusted the Pt loading from 0.6 to 2 wt % by repeating the synthesis up to 3 consecutive times. Figure 6a shows the sequence of the SCS reaction, where it is visible that the combustion front propagates very fast through the foam starting from the bottom side. The whole process is very fast coming to conclusion, being over in less than 10 min after up to 3 impregnation cycles (Fig. 6b). The physicochemical characterization enlightened a homogeneous catalytic layer covering the entire foam (Fig. 6c), with a Pt dispersion between 5 and 20% (the shorter the synthetic time, the higher the dispersion). The mean Pt crystallite size, measured by Rietveld method from XRD, and confirmed by TEM, is between 15 and 20 nm and is, thus, independent from the synthesis conditions (Fig. 6d). The adhesion of the thin coating layers was verified to be excellent: by stressing the coated foams in ultrasonic bath for 1 h, less than 0.1 wt % weight loss was recorded.

SCS TO PREPARE STRUCTURED CATALYSTS FOR ENERGY APPLICATIONS

Nowadays, the challenge is to move towards zero-emission energy sources. On this perspective, hydrogen is the most attractive energy carrier to be used in fuel cells, electrical vehicles, and electrical power plants, with zero, or near-to-zero emissions of greenhouse gases and hazardous species. Hydrogen, which unfortunately is not available in nature, can be produced via reforming processes from many hydrogen-containing molecules and fuels [147], or by electrolysis of water using renewable energy [148]. Thus, the interest of scientists lies in the production of syngas (a mixture of H_2 and CO) from the reforming of commonly available hydrocarbons. Steam reforming of natural gas on noble metal catalysts is the most widely used industrial process to produce syngas. Indeed, also the use of renewable fuels, such as biogas and light alcohols (methanol and ethanol) represents an interesting and relatively low-cost renewable source of hydrogen, since these fuels can be derived from biomass [149, 150]. As an energy source, also the catalytic combustion of hydrocarbons is an attractive solution for both industrial and domestic applications. The use of a catalyst for a combustion reaction promotes the full and efficient oxidation of hydrocarbons at temperatures far lower than those established in typical flame combustors, with high combustion efficiency. Thus, reaching the complete conversion of hydrocarbons at lower temperature, emissions of CO, unburned, and NO$_x$ are drastically reduced.
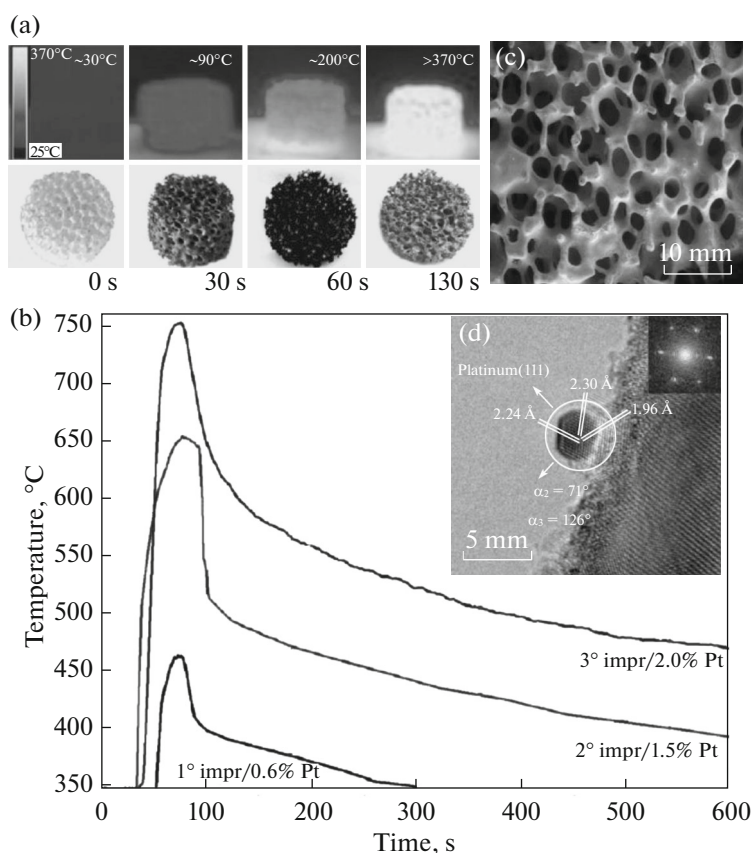
Fig. 6. Microwase-assisted SCS to deposit Pt onto alumina foams: (a) thermographs during the process and (b) temperature profiles during the process for three different impregnation steps; (c) low-magnification SEM of a coated foam after 3-min synthesis and (d) HRTEM of the 0.6% Pt/α-Al$_2$O$_3$ foam. Data rearranged from [55].

Focusing hydrogen production, Vita et al. [40, 42, 106] prepared both cordierite monoliths and alumina open cell foams by SCS for steam reforming, and oxy-steam reforming of methane and biogas to produce syngas. Concerning cordierite monoliths, they first deposited a thin layer of γ-Al$_2$O$_3$ [40] or CeO$_2$ [42] by SCS. They did this dipping the monoliths in a solution of aluminum nitrate [40] or cerium nitrate [42], and urea followed by placing the monoliths in an oven at 600°C for 2 h in calm air. Then, they deposited the active phase of the catalyst, Ru [40], Rh, Pt or Ni [42], by wet impregnation (dipping the monoliths in a solution containing the respective metal nitrate) and calcining for 2 h at 400°C in calm air. The deposition was repeated several times to reach various catalyst loadings (varying from 0.1 to 0.5 mg cm^{-2}, as noble metal deposited over the structure). All monoliths showed excellent mechanical resistance since the coated structures lost less than 0.3% of their weight when subjected to a double ultrasonic treatment in a water/acetone solution for 1 h, at 130 W and 45 kHz. Pressure drop measurements carried out at increasing superficial velocity, up to 15 m s^{-1}, denoted very low values, not exceeding 11 000 Pa m^{-1}, very similar to the values

measured on the bare monolith (indicative that the coated catalytic layer is very thin and it does not influence the pressure drop). Figure 7a shows a series of images of the monolith during the various phases of the coating process for the deposition of Ni/CeO$_2$. SEM images (Fig. 7b) show that the catalytic layer is very thin (as confirmed by pressure drop measurements), with uniform distribution along the walls and the corners. XRD measurements confirmed the composition of the desired catalyst deposited on the structure (Fig. 7c). Finally, a series of catalytic tests towards the reaction of oxy-steam reforming of CH$_4$ showed brilliant performance of the structured catalysts (Fig. 7d): in the case of Ni/CeO$_2$, it maintained a full conversion of CH$_4$ up to 180 000 NmL g$_{cat}^{-1}$ h^{-1}, with almost 75% of H$_2$ produced and a H$_2$/CO molar ratio equal to 3.2.

Using the procedure previously described, Vita et al. [106] deposited a 1.5% Rh/CeO$_2$ catalyst by SCS and wetness impregnation over Al$_2$O$_3$ open cell foams. They compared the performance of 30 and 40 ppi Rh/CeO$_2$ foams and a 400 cpsi monolith towards the oxy-steam reforming reaction (also known as tri-reforming reaction) of synthetic biogas. The SCS
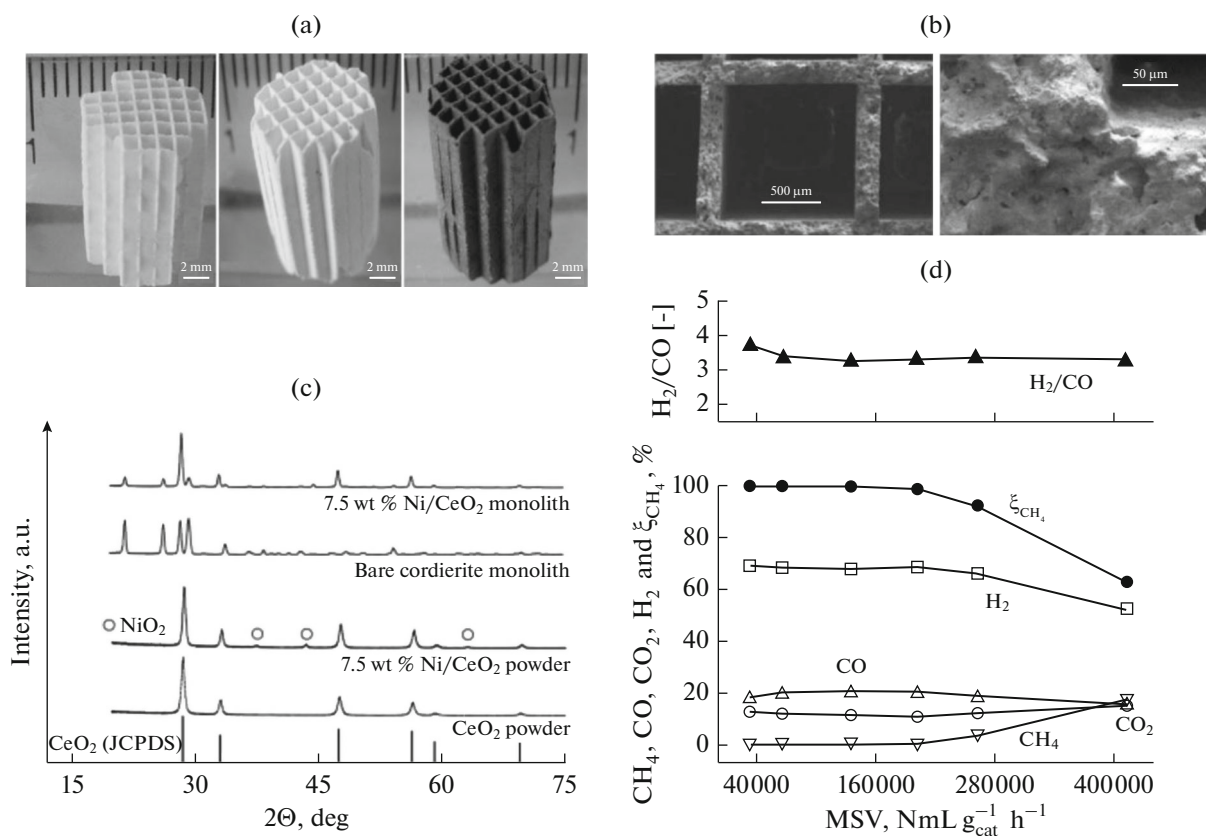
(a)

(b)

(c)

(d)

Fig. 7. (a) Cordierite monolith uncoated, coated with CeO_2 by SCS, and with Ni by wetness impregnation; (b) SEM images of the Ni/CeO_2 monolith; (c) XRD patterns of CeO_2 and Ni/CeO_2 powders, cordierite monolith and Ni/CeO_2 monolith; and (d) performance of Ni/CeO_2 monolith towards the oxy-steam reforming of methane as a function of the weight space velocity at $T =$ 800°C, O/C = 0.55, and S/C = 1.2. Data rearranged from [40].

deposition produced a very thin catalytic layer, with a specific surface area of 14 m^2 g^{-1}, and Rh dispersion of 22%. Figure 8a shows pictures for the 40 ppi foam after CeO_2 and Rh/CeO_2 deposition: the catalytic layer appears uniformly distributed on the whole surface of the foam. Figure 8b shows SEM images with EDX mapping, again, the catalyst is homogeneous, completely covering the surface. On top of this, EDX mapping confirms that both Ce and Rh, the active element of the catalyst, are highly homogeneously dispersed. The comparison of the catalytic activity between the monolith and the foam (Figs. 8c, 8d) proves the better performance of the foam over the monolith. In fact, the foam is able to maintain a full CH_4 conversion, and a constant 50% CO_2 conversion, for the whole range of weight space velocity (up to 280 000 NmL g$_{cat}^{-1}$ h^{-1}), while the monolith decreases the performance when the weight space velocity exceed 80 000 NmL g$_{cat}^{-1}$ h^{-1}). The coated foam allows for an almost constant H_2/CO molar ratio close to 1.74, while the monolith exhibits a decreasing value from 1.39 to 1.32 with the weight space velocity.

Another way to produce hydrogen is via the decomposition of light alcohols. In particular, ethanol decomposition in the presence of nickel-based catalysts represents an easy way to extract hydrogen. The use of a porous support can increase the surface area of the active phase of a catalyst, and thus enhances its structural and thermal stability. Cross et al. [107] demonstrated this effect preparing a series of Ni supported catalysts on γ-Al_2O_3 pellets with a ring geometry (internal/external diameter: 0.1/0.25 in) for the selective decomposition of ethanol to hydrogen. They prepared the supported catalysts by dipping γ-Al_2O_3 pellets in aqueous solution of nickel nitrate hexahydrate and glycine where ϕ = 1.75, with a varied immersion time from 1 s to 30 min. After a drying period of 24 h, the impregnated catalysts were placed on a hot plate at 500°C to initiate the ignition of the combustion reaction. Figure 9a shows the combustion front propagation as captured by an IR camera; in less than 1 min the combustion reaction is over. The peak temperature reached during the combustion reaction depends on the impregnation time, that is, on the amount of solution the γ-Al_2O_3 pellets adsorbed, as shown in Fig. 9b: the longer the impregnation time,
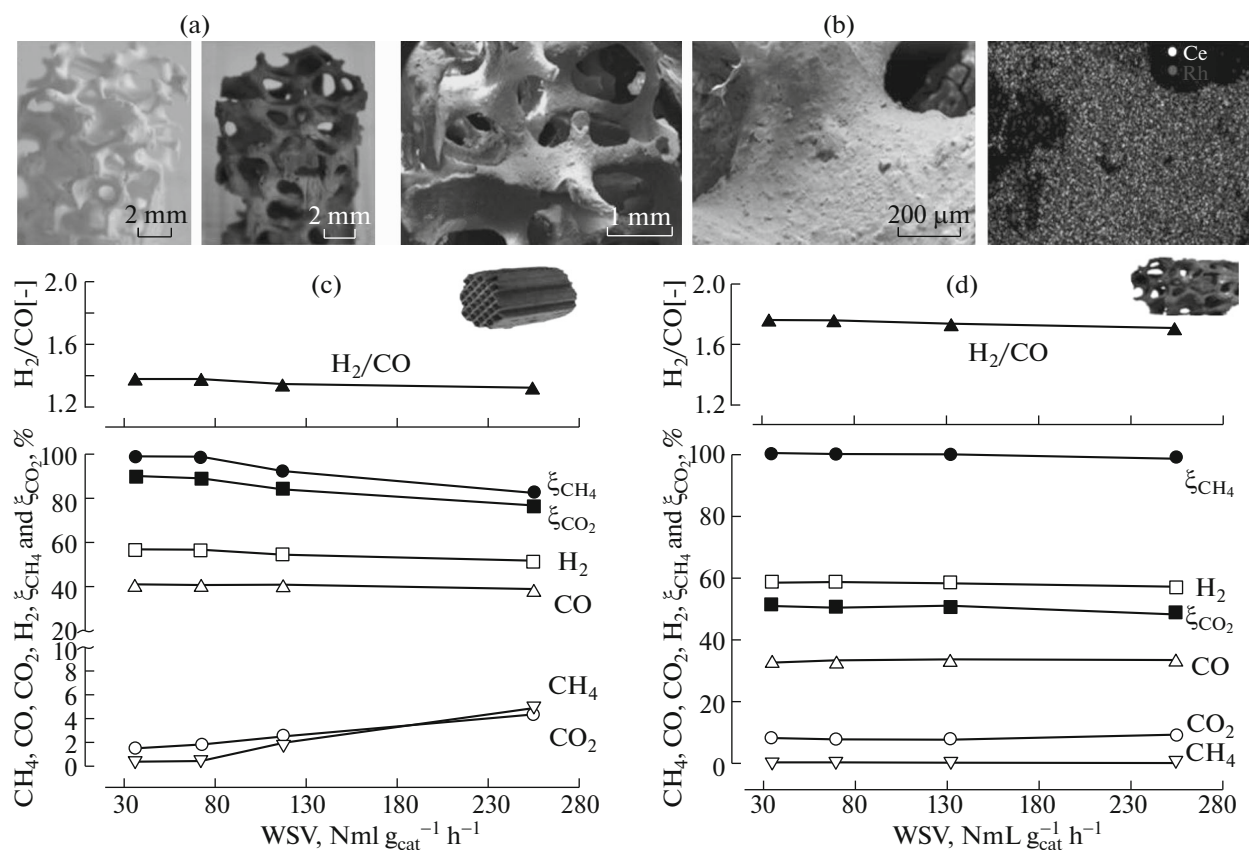
Fig. 8. (a) 40 ppi alumina open cell foam coated with CeO_2 by SCS, and with Rh by wetness impregnation; (b) SEM images of the Rh/CeO_2 foam with EDX mapping; and performance of Rh/CeO_2 monolith (c) and Rh/CeO_2 open cell foam (d) towards the oxy-steam reforming of biogas as a function of the weight space velocity at $T = 900°C$ (for the monolith: $S/C = 0.3$ and $O/C = 0.1$; for the open cell foam: $S/C = 0.1$ and $O/C = 0.2$). Data rearranged from [106].

the higher the peak temperature and the shorter the reaction time. A series of SEM characterizations demonstrated that Ni was deposited as a thin layer on the surface of γ-Al_2O_3 pellets. This is due to the alumina support, the impregnated support, and the supported catalysts all appearing very similar (Fig. 9c). In fact, the supported catalysts exhibit a uniform nanostructure with agglomerates smaller than the impregnated catalysts. The authors evaluated the catalytic activity towards the reaction of ethanol decomposition in a fixed bed configuration using a quartz tube reactor. Before testing, the catalysts were reduced in situ in a pure hydrogen flow rate at 300°C for 1 h. The catalytic decomposition of ethanol was investigated over a flow rate of 140 cm^3 min^{-1} of nitrogen saturated with ethanol at 0°C, containing 3.8% ethanol and O_2/C_2H_5OH molar ratio of 0.5. Figures 9d and 9e show ethanol conversion and hydrogen selectivity for the supported Ni/γ-Al_2O_3 catalysts impregnated for 5 s and 1 min, respectively, in comparison with the blank support. The γ-Al_2O_3 exhibits complete ethanol conversion at lower temperature than the Ni-impregnated catalysts, but is also totally non-selective for H_2. This

means that the products of the reaction are water and ethylene. The catalyst impregnated for 5 s has a good activity for ethanol conversion but low values of H_2 selectivity, while the catalyst impregnated for 1 min has an opposite behavior. These results mean that the 5-s catalyst produces more water and ethylene than the 1-min catalyst, but less hydrogen and acetaldehyde. These results can be explained by the lower amount of Ni that was deposited on the 5-s catalyst compared to the 1-min one. In fact, the reaction of ethanol to water and ethylene is favored on alumina sites, while the reaction to acetaldehyde and hydrogen is favored in the presence of Ni. A higher dispersion of Ni is attained on the catalysts that were impregnated for 1 min. These results clearly demonstrate that SCS allows for control of the distribution of the active sites of a catalyst (that is, favoring different reaction pathways involved in a multiple step-reaction process) by varying the parameters governing the combustion process; such as the amount of solution impregnated onto the support, and the temperature at which the combustion reaction occurs. This in turns reflects how SCS can be used to drive a reaction towards the desired final products, hydrogen in this case.
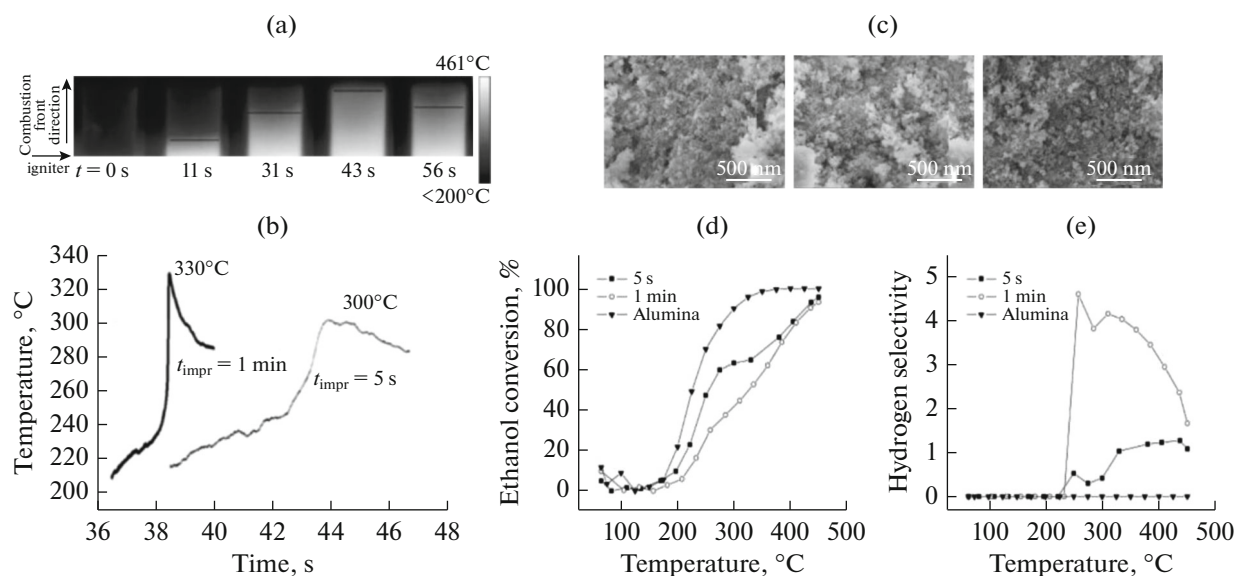
Fig. 9. Propagation of the combustion front taken by IR camera (a). Temperature profile of combustion front for samples prepared with 5 s and 1 min impregnation (b). SEM images of Al_2O_3 support, impregnated support, and supported catalyst (c). Ethanol conversion (d) and hydrogen selectivity (e) for samples prepared with 5 s and 1 min impregnation, and the original support. Data rearranged from [107].

Regarding the catalytic combustion of hydrocarbons, Tacchino et al. [37, 126] proposed and investigated new type of structured catalysts for the combustion of CH_4/H_2 mixtures at different molar ratios in lean conditions. The catalysts consisted of $Pd/NiCrO_4$, $Pd/CeO_2 \cdot ZrO_2$, and $Pd/LaMnO_3 \cdot ZrO_2$ lined over SiC monoliths. The authors prepared the structured catalysts using one-shot SCS, by dipping the ceramic monolith supports in homogeneous aqueous solutions. These solutions contained the metal–nitrate compounds, as oxidizers, and urea (for the preparation of $NiCrO_4$ and Al_2O_3) or glycine (for the preparation of $CeO_2 \cdot ZrO_2$ and $LaMnO_3 \cdot ZrO_2$) as fuel, along with Pd nitrate in the desired amount. The SCS reaction began in an oven set at 600°C. One-shot SCS allows for the reduction of the manufacturing time of structured catalysts, since all the precursors are mixed together before the initial combustion reaction. Figure 10a shows the general aspect of the structured catalyst wrapped with a vermiculite foil, to better fix it into the reactor. Figure 10b shows SEM images which reveal a very thin and uniform layer of $Pd/NiCrO_4$ catalyst covering the walls of the monolith. In particular, it is evident that the porous structure of the catalyst is due to the gases generated by the decomposition of the reacting precursors. The BET specific surface area increased from 0.2 (base SiC monolith) to 2.2 $m^2 g^{-1}$ measured on the coated $Pd/NiCrO_4$ structured catalyst. The catalytic activity was evaluated where the structured catalysts generated an overall power density of 7.6 $MW m^{-3}$. This power density was reached by first burning only CH_4 (5% vol

CH_4 in air with $\lambda = 2$), then only H_2 (17 vol % H_2 in air with $\lambda = 2$), then three different CH_4/H_2 lean mixtures at increased H_2 concentration at constant $\lambda = 2$ (see Fig. 10b) The overall flow rate was equal to 200 NmL min^{-1}, equivalent to a gas hourly space velocity of 16 000 h^{-1}. Among the various structured catalysts, the best results belonged to the $Pd/NiCrO_4$ catalyst, as shown in Fig. 10c. The SiC monolith reduced the methane half-conversion and light-off temperatures, when compared to the bare counterpart, for all the tested CH_4/H_2 mixtures. The addition of H_2 into the reactive mixture favored CH_4 combustion, in that the higher the H_2 concentration lowered the half-conversion and light-off temperatures (Fig. 10c, Mix 3). The presence of the catalyst also reduced CO emissions, where the recorded CO peak decreased with increasing H_2 concentration.

SCS TO PREPARE STRUCTURED CATALYSTS FOR POLLUTION CONTROL

The abatement of pollutants is one of the biggest challenges in modern society. Pollutant emissions damage our air, water, and soil which compromise the quality of life of this planet.

The particulate matter emitted by diesel engines is a critical issue in urban areas. On top of this, diesel engines produce dangerous NO_x. Notwithstanding these drawbacks, diesel engines are attractive for their efficiency and durability. Diesel engine emission level standards are always more stringent due to European regulations. A promising approach to lower diesel
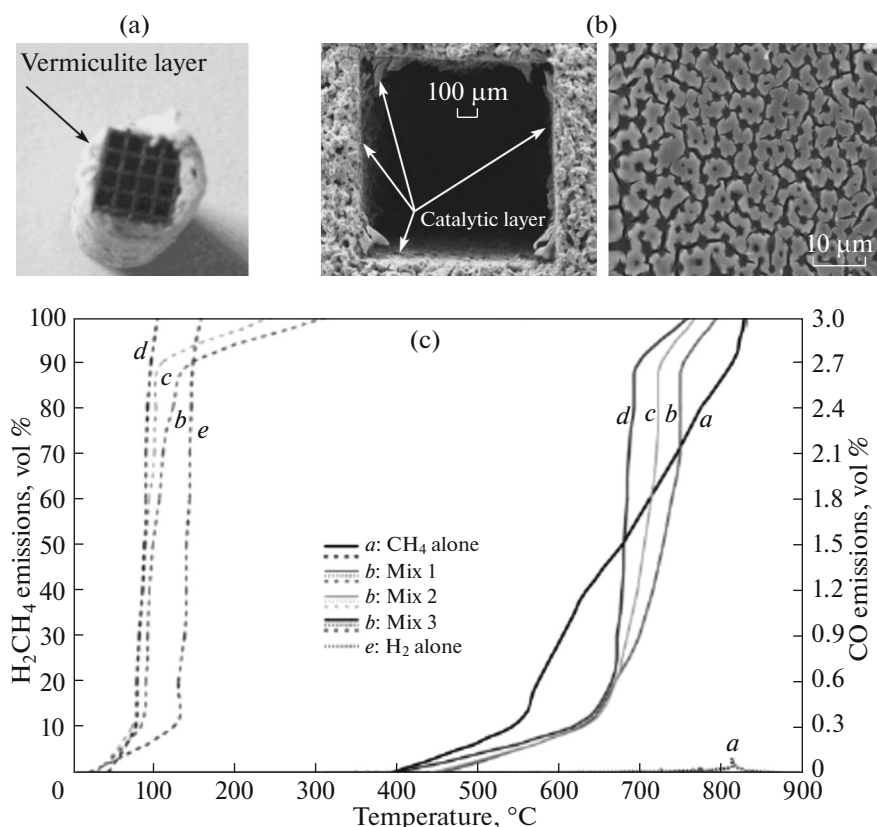
Fig. 10. (a) Picture of a SiC structured catalyst wrapped in a vermiculite foil; (b) SEM images of the SiC monolith lined with Pd/NiCrO$_4$: frontal view of a microchannel and internal surface covered by a spongy layer of catalyst; and (c) catalytic performance of the SiC monolith lined with Pd/NiCrO$_4$: CH$_4$ conversion (solid lines), H$_2$ conversion (broken lines), and CO emissions (dotted lines) vs. T as a function of the reactive mixture (a: CH$_4$ alone; b: Mix 1 CH$_4$/H$_2$ molar ratio 75/25; c: Mix 2 CH$_4$/H$_2$ molar ratio 50/50; d: Mix 3 CH$_4$/H$_2$ molar ratio 25/75; e: H$_2$ alone). Data rearranged from [37].

emissions comes from the use of specific catalytic traps, able to concomitantly reduce particulate matter and NO$_x$. Particulate filters are made of temperature-resistant porous material, such as ceramics, with an as-high-as-possible filtration area so as to decrease the pressure drop and the related fuel penalty. For this purpose, Fino et al. [71] deposited a perovskite catalyst, LaCr$_{0.9}$O$_3$, on wall-flow traps used as a support, through use of SCS. They used both cordierite and silicon carbide as supports. The supports were dipped in a solution of La and Cr nitrates, with urea as a fuel, and placed in an oven at 600°C for few minutes. The dipping and heating procedure was repeated until 10% in weight of the catalyst was deposited. Figure 11a shows the SEM characterization of a cordierite trap coated with LaCr$_{0.9}$O$_3$. The catalyst appears to be strongly bonded to the support, additionally the microstructure seems to have a spongy morphology as a consequence of the evolved gases from the SCS reaction. This feature represents a great advantage as it favors the contact between the catalyst and soot that accumulates within the trap. The catalytic activity of the developed catalytic traps was tested in a pilot plant connected with a diesel engine, to better simulate die-

sel exhaust gases. Each prepared trap was first loaded with a low temperature exhaust gas (about 200°C) until a pressure drop of 110−160 mbar was reached (corresponding to a particulate hold-up of about 10 g L^{-1}). Once complete, trap regeneration was induced by post injecting diesel fuel, with a metering pump, in the exhaust gases, and burning the resulting gases in an oxidizing honeycomb catalyst (OXICAT by Johnson Matthey) placed just upstream from the trap. The time needed for completing trap regeneration (e.g., combustion of the soot hold-up) is indicative of the catalyst performance; the higher the catalyst activity, the less amount of time required. Figure 11b shows the activity of a catalyzed cordierite trap compared to a non-catalyzed wall-flow trap. The regeneration was achieved only for the structured catalyst at about 600°C. Figure 11c shows a direct observation of the non-catalytic and catalytic traps, enlightening that the regeneration is not complete. In fact, soot combustion starts in the centre of the structure, where the hot-gases concentrated their flow with lower pressure drop and higher temperature. However, the regenerated zone is larger for the catalytic trap than for the non-catalytic one. Interestingly, the catalytic trap made
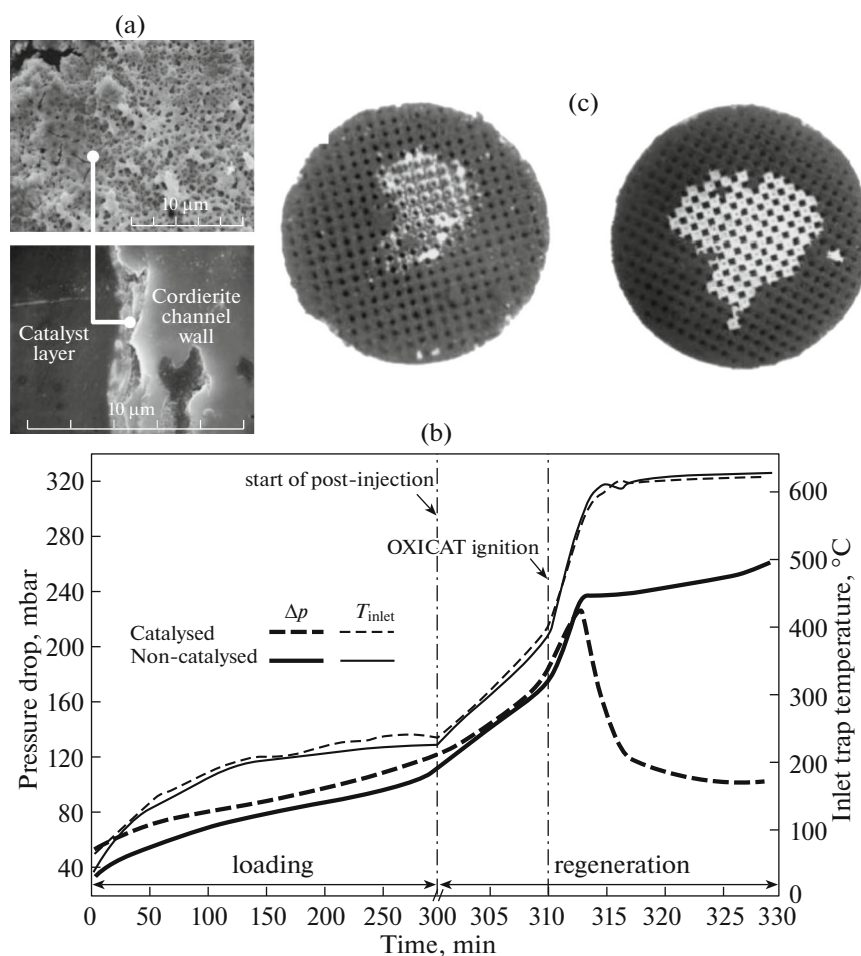
Fig. 11. (a) SEM images of a cordierite wall-flow trap coated with $LaCr_{0.9}O_3$; (b) soot loading and regeneration cycles for a catalytic ($LaCr_{0.9}O_3$) and a non-catalytic wall-flow cordierite trap; and (c) images of the inlet side of a non-catalytic (left) and $LaCr_{0.9}O_3$ catalytic (right) cordierite wall-flow monoliths after regeneration. Data rearranged from [71].

with SiC resulted fully regenerated. This effect was explained by the higher thermal conductivity of SiC ($55 \, W \, m^{-1} \, K^{-1}$) compared to cordierite ($2.8 \, W \, m^{-1} \, K^{-1}$). In fact, the 20 times higher value of thermal conductivity of SiC favors the transfer of the heat, released by soot combustion, to adjacent channels. This then ignites regeneration step and completes the regeneration throughout the entire trap.

Volatile organic compounds (VOC) are a large group of low molecular-weight organic chemicals that are emitted from a great variety of sources; such as industrial processes, transport, household activities, and so on. Catalytic oxidation is considered to be one of the most effective techniques for VOC removal. This is because the total oxidation of diluted fuels occurs at relatively low temperatures leading to low emissions of NO_x and unburned fuels. For this purpose, Piumetti et al. [77] recently synthesized Mn_3O_4-based structured catalysts based on cordierite monoliths, by SCS. They dipped cylindrical cordierite honeycombs in a solution of Mn nitrate and glycine, and placed the impregnated supports in an oven at 500°C for 30 min. The procedure was repeated until 0.48 g of catalyst was deposited on each monolith. Figure 12a shows the difference between a bare and a coated monolith, whereas the SEM images illustrate the thin, spongy catalyst layer that is uniformly distributed along the walls of the monolith. Catalytic tests were carried out in a stainless-steel reactor, heated in a horizontal split tube furnace, by feeding a reactive mixture (containing 1000 ppm of ethylene, propylene, and toluene, 10 vol % oxygen, and nitrogen to balance). The catalytic reaction started when the structured catalyst reached a temperature of 100°C, then it reached full VOC oxidation at 310°C, as shown in Fig. 12b. The excellent catalytic activity was maintained, even increasing the gas hourly space velocity up to four times, which is fundamental for process intensification. The good catalytic activity of Mn_3O_4 was ascribed to the abundantce of Brønsted acidic Mn–OH sites, which are beneficial for the total oxidation of
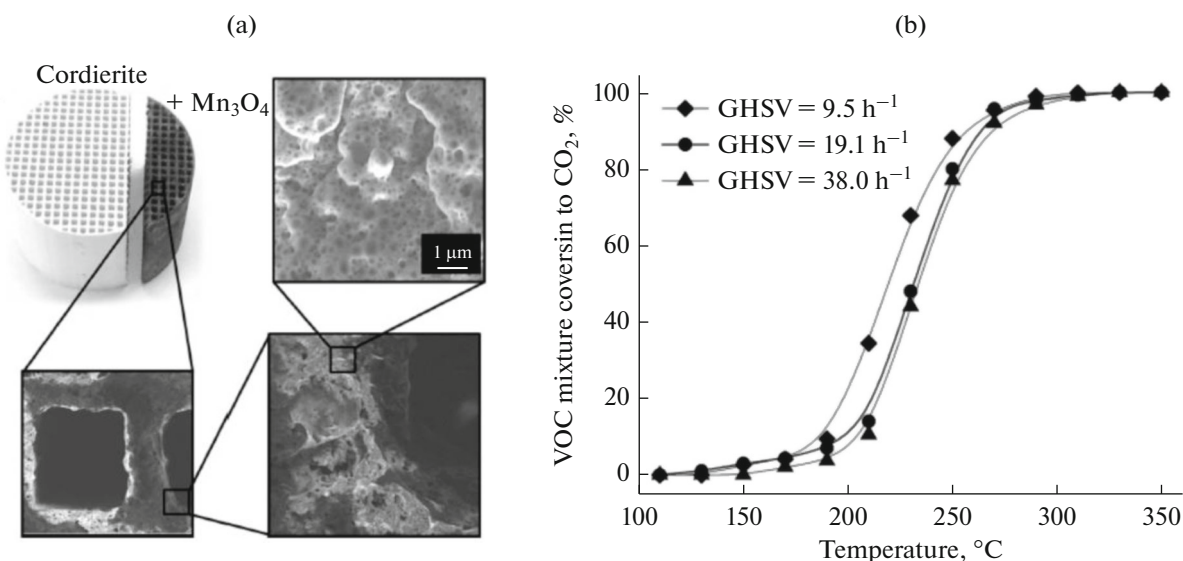
(a)   (b)

Fig. 12. (a) Picutre and SEM images of a cordierite monolith coated with Mn_3O_4 and (b) catalytic performance of a monolith coated with Mn_3O_4 for the total oxidation of a VOC mixture (1000 ppm mixture of ethylene, propylene, and toluene, 10 vol % O_2, N_2 = balance) at different gas hourly space velocity. Data rearranged from [77].

VOC, since they are responsible for the adsorption/desorption rates of both reactants and products.

Methane is generated by various human activities, such as natural gas engines or coal mines. Methane is the second most abundant greenhouse gas, where it can trap about 20 times more heat than CO_2 and its presence in the atmosphere affects the climate. The abatement of methane emissions lies in the activation of the C−H bonds, which requires high temperature and leads to radical reactions that have low intrinsic selectivity. Thus, catalytic combustion represents a promising option to oxidize nearly 100% of methane, in the exhaust stream, at temperatures below 400°C. Ercolino et al. [45, 46] prepared a series of structured Pd/Co_3O_4 catalysts using open cell foams made of alumina, zirconia, and carborundum, comparing their performance against an alumina monolith. All structured catalysts were prepared via SCS, to coat a thin layer of Co_3O_4, followed by wet impregnation to deposit Pd, to ensure that all Pd was available on the surface of Co_3O_4. First, all structures were cleaned with a solution of water/acetone. The authors dipped each structure in a 3 M solution of Co nitrate and glycine, with $\phi = 0.25$. After removing the solution in excess, the impregnated structures were placed in an oven at 250°C for 15 min. The operation was repeated several times to reach an amount of Co_3O_4 equal to 200 mg. The structures were then calcined at 600°C for 4 h in calm air. After this, 3 wt % palladium was deposited by dipping the structure into a solution containing Pd nitrate, followed by calcining again at 600°C for 4 h in calm air. Adhesion tests carried out on both the coated monoliths and foams, demonstrated excellent stability of the catalytic coating, showing a weight loss of 0.7−1.4 wt % after 1 h sonication (depending on the geometrical properties of the foams [46]). The structured catalysts were tested towards the lean combustion of methane by feeding 0.5 and 1 vol% of methane in nitrogen, with a constant oxygen-to-methane molar ratio equal to 8, at different weight hourly space velocity (WHSV = 30, 60, and 90 NL h^{-1} g_{cat}^{-1}).

Figure 13a shows the catalytic activity of all foams (30 ppi) and the monolith, with $CH_4 = 0.5\%$ and WHSV = 30 (bare structures visible in Fig. 13b), along with the activity of pure Pd/Co_3O_4 powder for reference. The three structured foams show better catalytic performance compared to the pure Pd/Co_3O_4 powder, which is better than the performance of the catalyzed monolith. In particular, among the three types of foams, the better performance belongs to the zirconia catalyzed one. In fact, the coated zirconia can reach full methane conversion below 350°C at 30 WHSV. When WHSV is increased, the performance of all foams worsen slightly, with the order of reactivity being zirconia > alumina > carborundum. The better performance of zirconia foams can be explained considering their lower volumetric heat exchange coefficients, which favor the reaction heat removal by convection via the flue gases. Figure 13c shows SEM images of Pd/Co_3O_4 as a powder and as a layer on the foams; the comparison of the two images shows the same truncated octahedron crystals, typical of the Co_3O_4 spinel material. This is a clear sign that SCS allows for the preparation of the desired catalytic materials, not only, at powder level, but at structured level, as well. From the preliminary catalytic screening, the best structured catalyst (the coated zirconia 30 ppi), was exposed to a repetitive series of catalytic tests
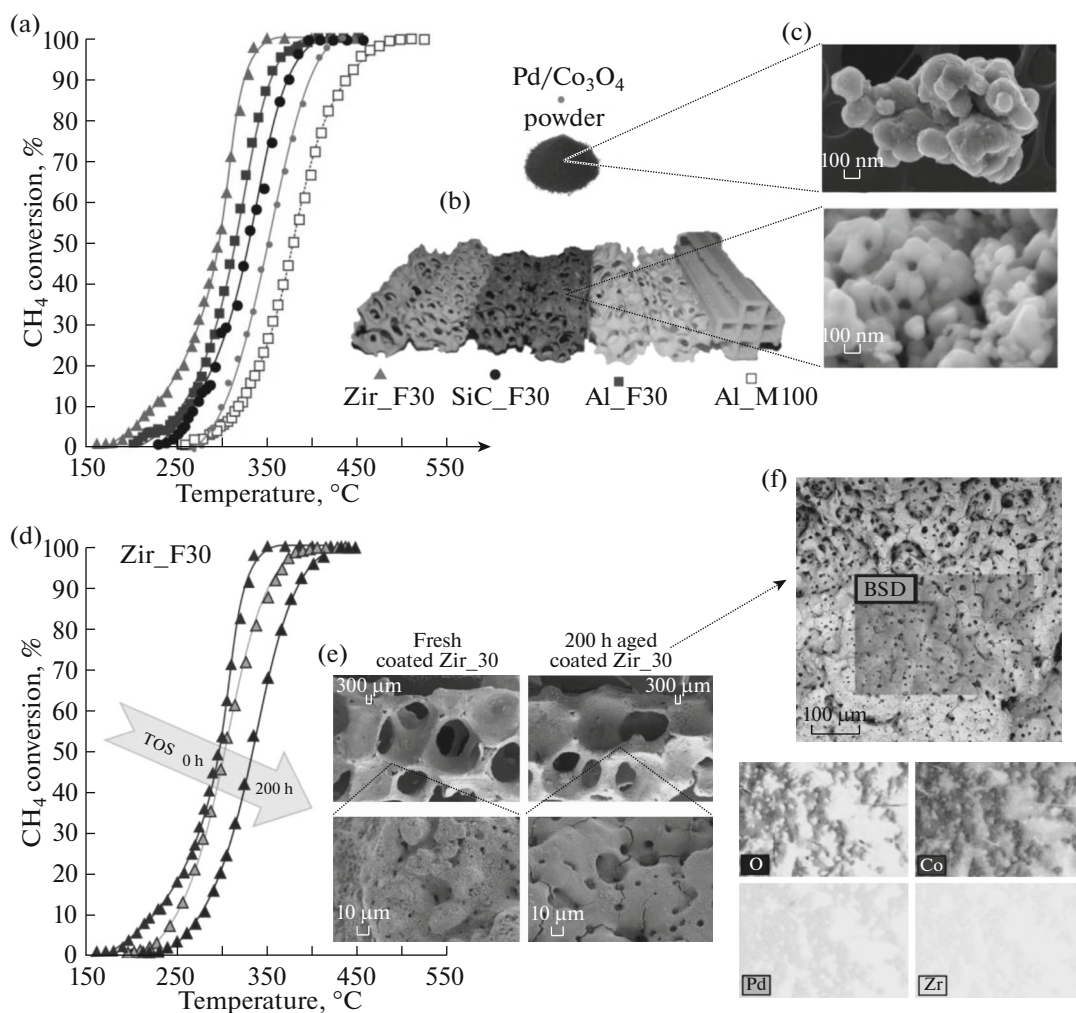
Fig. 13. (a) Catalytic performance of various 30 ppi foams (zirconia, carborundum, and alumina) and a 100 cpsi alumina monolith coated with 3% Pd/Co_3O_4 for the lean combustion of methane in lean conditions (0.5% CH_4, λ = 2, weight hourly space velocity = 30 NL h^{-1} g$_{cat}^{-1}$); (b) images of the bare structures used as a support and of the Pd/Co_3O_4 powder; (c) FESEM images of Pd/Co_3O_4 as powder and lined over the structrured catalyst; (d) catalytic performance of the 3% Pd/Co_3O_4 coated 30 ppi zirconia foam after 0, 20, and 200 h of TOS at 400 °C in lean combustion conditions (0.5% CH_4, λ = 2, weight hourly space velocity = 30 NL h^{-1} g$_{cat}^{-1}$); (e) FESEM images of Pd/Co_3O_4 lined over the structured zirconia catalyst after 0 and 200 h TOS; and (f) SEM/EDS overall and combined mapping of 3 wt % Pd/Co_3O_4 on zirconia foam after 200 h TOS. Data partially rearranged from [45, 46].

for an overall time-on-stream (TOS) of 200 h, with a series of start/stop. Specifically, the reactor was fed with a reactive mixture containing 0.5 vol % methane at 30 WHSV, maintaining a combustion temperature fixed at 400°C. Figure 13d shows excellent results of the catalytic activity in fresh conditions, and after 20 and 200 h of TOS. After 200 h TOS, the shift of the methane conversion curve towards higher temperatures is very limited, and the structured catalyst can fully convert methane at temperatures below 400°C. Figure 13e shows FESEM images of the fresh and used (after 200 h TOS) foams, made up of structured zirconia coated with Pd/Co_3O_4. The comparison of the images enlightens a variation of the morphology of the catalytic layer. In particular, the surface of the aged catalyst appears highly corrugated, with lots of cracks, mainly due to the long-time exposure at relatively high temperature. The apparent increase of the specific surface area is due to the surface roughening and could on one hand reduce palladium dispersion, explaining thus the reduction of the performance, but on the other hand it may enhance the adsorption of product molecules, thus favoring conversion and limiting the decrease in activity. Figure 13f shows SEM/EDS mapping of the surface of the aged catalyst, enlightening homogeneity and good distribution of each element

(O, Co, and Pd). The average weight percentage of Pd, 3.75%, is close to the theoretical value of 3%, with small variations depending on the measured area (atomic Pd/Co ratio variable from 0.034 to 0.039).

The presence of Zr in the elemental mapping image strongly suggest that the thickness of the catalytic coating is very thin, less than 50 μm. This is a clear demonstration that deposition of catalysts via SCS, on ceramic supports, is a viable way to synthesize structured catalysts.

OUTLOOK AND FUTURE PERSPECTIVES

Solution combustion synthesis (SCS) is a preparation method for inorganic materials of any nature and shape. This technique was first described at the end of the 1960s, as the solid-flame combustion for the preparation of ceramic and intermetallic compounds. Over the past five decades, SCS become an effective economical process with short reaction times and low energy requirements, needed only during the initial ignition step of the combustion reaction. Moreover, SCS requires relatively cheap reactants, simple equipment, and low-cost facilities, allowing the reduction of production costs, compared to conventional manufacturing processes. These facts imply that energy production must be increased, while managing the unceasing requirements of new products, all while taking care of the environment. Thus, SCS can be envisaged as a manufacturing technique that perfectly suits the requirements of process intensification, such as cleaner, safer, smaller, and more energy-efficient matters. The intrinsic energy-saving and high purity of the desired products make SCS an attractive, innovative, and intriguing technique to produce structured catalysts. The process is easily scaled up to any kind of size, and type of application. Until now, SCS has been used to produce different materials, such as advanced ceramics, catalysts, pigments, composites, intermetallic, nanomaterials, and structured catalysts, with reproducible safe mass productions at a lab-scale up to 1 kg of nano-materials per hour [11, 12]. All the cases reported in this mini-review showed that SCS is a good technique to deposit catalysts on various structures different for geometry (monoliths, spheres, foams, etc.) and materials (cordierite, alumina, zirconia, silicon carbide, iron, etc.). Moreover, these structured catalysts exhibit good performance for different applications, such as syngas production via biogas reforming or ethanol decomposition; methane oxidation; soot, NO_x, and VOC abatement, to name a few examples.

Lastly, SCS presents some disadvantages, among all, being the formation of NO_x during the combustion reaction [18, 20, 28, 48, 49, 53]. Metal nitrate precursors can undergo partial thermal oxidation, thus releasing NO_x, and the organic fuels that contain nitrogen atoms (urea, glycine, β-alanine, etc.) that decompose to generate NO_x. Besides this, being the thermal decomposition of N-containing molecules is limited, and only small amounts of NO_x are released, at the lab-scale. Surely, in the case of industrial scale-up, NO_x emissions can represent a critical environmental issue. In this case, a specific selective catalytic reduction plant, with ammonia, must be considered. This critical problem could be overcome by carefully, and strategically, selecting the organic fuels necessary to ignite the combustion reaction. In fact, just as an example, the use of glycerol (a free-N containing molecule) as a fuel is particularly interesting to reduce NO_x emissions [53].

In the end, the SCS method can be considered as a viable, inexpensive, environmentally-friendly, energy saving, and safe manufacturing process used to synthetize structured catalysts for many different applications.

ACKNOWLEDGEMENTS

REFERENCES

1. Rogachev, A.S., Shugaev, V.A., Kachelmyer, C.R., and Varma, A., Mechanisms of structure formation during combustion synthesis of materials, *Chem. Eng. Sci.*, 1994, vol. 49, no. 24, pp. 4949–4958. doi 10.1016/0009-2509(94)00389-0

2. Merzhanov, A.G., Fluid dynamics phenomena in the processes of self-propagating high-temperature synthesis, *Combust. Sci. Technol.*, 1995, vol. 105, nos. 4–6, pp. 295–325. doi 10.1080/00102209508907756

3. Gillan, E.G. and Kaner, R.B., Synthesis of refractory ceramics via rapid metathesis reactions between solid-state precursors, *Chem. Mater.*, 1996, vol. 8, no. 2, pp. 333–343. doi 10.1021/cm950232a

4. Patil, K.C., Aruna, S.T., and Ekambaram, S., Combustion synthesis, *Curr. Opin. Solid State Mater. Sci.*, 1997, vol. 2, no. 2, pp. 158–165. doi 10.1016/S1359-0286(97)80060-5

5. Varma, A., Rogachev, A.S., Mukasyan, A.S., and Hwang, S., Combustion synthesis of advanced materials: Principles and applications, *Adv. Chem. Eng.* 1998, vol. 24, no. C, pp. 79–226. doi 10.1016/S0065-2377(08)60093-9

6. Kingsley, J.J. and Patil, K.C., A novel combustion process for the synthesis of fine particle α-alumina and related oxide materials, *Mater. Lett.*, 1988, vol. 6, no. 11, pp. 427–432. doi 10.1016/0167-577X(88)90045-6

7. Kirchnerova, J. and Klvana, D., Synthesis and characterization of perovskite catalysts, *Solid State Ionics*, 1999, vol. 123, no. 1, pp. 307–317. doi 10.1016/S0167-2738(99)00102-2

8. Kaliaguine, S., van Neste, A., Szabo, V, Gallot, J.E., Bassir, M., and Muzychuk, R., Perovskite-type oxides

synthesized by reactive grinding: I. Preparation and characterization, *Appl. Catal. A: Gen.*, 2001, vol. 209, no. 1, pp. 345–358. doi 10.1016/S0926-860X(00)00779-1

9. Patil, K.C., Aruna, S.T., and Mimani, T., Combustion synthesis: An update, *Curr. Opin. Solid State Mater. Sci.*, 2002, vol. 6, no. 6, pp. 507–512. doi 10.1016/S1359-0286(02)00123-7

10. Porcu, M., Orrù, R., Cincotti, A., and Cao, G., Self-propagating reactions for environmental protection: Treatment of wastes containing asbestos, *Ind. Eng. Chem. Res.*, 2005, vol. 44, no. 1, pp. 85–91. doi 10.1021/ie040058c

11. Mukasyan, A.S. and White, J.D.E., Combustion joining of refractory materials, *Int. J. Self-Propag. High-Temp. Synth.*, 2007, vol. 16, no. 3, pp. 154–168. doi 10.3103/S1061386207030089

12. Mukasyan, A.S. and Dinka, P., Novel approaches to solution-combustion synthesis of nanomaterials, *Int. J. Self-Propag. High-Temp. Synth.*, 2007, vol. 16, no. 1, pp. 23–35. doi 10.3103/S1061386207010049

13. McCauley, J.W. and Puszynski, J.A., Historical perspective and contribution of US researchers into the field of self-propagating high-temperature synthesis (SHS)/combustion synthesis (CS): Personal reflections, *Int. J. Self-Propag. High-Temp. Synth.*, 2008, vol. 17, no. 1, pp. 58–75. doi 10.3103/S106138620801007X

14. Rogachev, A.S. and Baras, F., Models of SHS: An overview, *Int. J. Self-Propag. High-Temp. Synth.*, 2007, vol. 16, no. 3, pp. 141–153. doi 10.3103/S1061386207030077

15. Merzhanov, A.G. and Borovinskaya, I.P., Historical retrospective of SHS: An autoreview, *Int. J. Self-Propag. High-Temp. Synth.*, 2008, vol. 17, no. 4, pp. 242–265. doi 10.3103/S1061386208040079

16. Borisova, A.L. and Borisov, Y.S., Self-propagating high-temperature synthesis for the deposition of thermal-sprayed coatings, *Powder Metall. Met. Ceram.*, 2008, vol. 47, no. 1, pp. 80–94. doi 10.1007/s11106-008-0012-5

17. Yermekova, Z., Mansurov, Z., and Mukasyan, A.S., Combustion synthesis of silicon nanopowders, *Int. J. Self-Propag. High-Temp. Synth.*, 2010, vol. 19, no. 2, pp. 94–101. doi 10.3103/S1061386210020032

18. Specchia, S., Finocchio, E., Busca, G., and Specchia, V., Combustion Synthesis, in *Handbook of Combustion*, Lackner, M., Winter, F., and Agarwal, A.K., Eds., Weinheim: Wiley–VCH, 2010, pp. 439–472. doi 10.1002/9783527628148.hoc088

19. Shteinberg, A.S., Berlin, A.A., Denisaev, A.A., and Mukasyan, A.S., Kinetics of fast reactions in condensed systems: Some recent results (An autoreview), *Int. J. Self-Propag. High-Temp. Synth.*, 2011, vol. 20, no. 4, pp. 259–265. doi 10.3103/S1061386211040030

20. Specchia, S., Galletti, C., and Specchia, V., Solution combustion synthesis as intriguing technique to quickly produce performing catalysts for specific applications, *Stud. Surf. Sci. Catal.*, 2010, vol. 175, pp. 59–67. doi 10.1016/S0167-2991(10)75008-4

21. Liu, G., Li, J., and Chen, K., Combustion synthesis of refractory and hard materials: A review, *Int. J. Refract.*

22. Rosa, R., Veronesi, P., and Leonelli, C., A review on combustion synthesis intensification by means of microwave energy, *Chem. Eng. Process. Process Intensif.*, 2013, vol. 71, pp. 2–18. doi 10.1016/j.cep.2013.02.007

23. González-Cortés, S.L. and Imbert, F.E., Fundamentals, properties, and applications of solid catalysts prepared by solution combustion synthesis (SCS), *Appl. Catal. A: Gen.*, 2013, vol. 452, pp. 117–131. doi 10.1016/j.apcata.2012.11.024

24. Wen, W. and Wu, J.-M., Nanomaterials via solution combustion synthesis: A step nearer to controllability, *RSC Adv.*, 2014, vol. 4, no. 101, pp. 58090–58100. doi 10.1039/C4RA10145F

25. Ghose, R., Hwang, H.T., and Varma, A., Oxidative coupling of methane using catalysts synthesized by solution combustion method: Catalyst optimization and kinetic studies, *Appl. Catal. A: Gen.*, 2014, vol. 472, pp. 39–46. doi 10.1016/j.apcata.2013.12.004

26. Mukasyan, A.S., Rogachev, A.S., and Aruna, S.T., Combustion synthesis in nanostructured reactive systems, *Adv. Powder Technol.*, 2015, vol. 26, no. 3, pp. 954–976. doi 10.1016/j.apt.2015.03.013

27. Pawade, V.B., Swart, H.C., and Dhoble, S.J., Review of rare earth activated blue emission phosphors prepared by combustion synthesis, *Renew. Sustain. Energy Rev.*, 2015, vol. 52, pp. 596–612. doi 10.1016/j.rser.2015.07.170

28. Varma, A., Mukasyan, A.S., Rogachev, A.S., and Manukyan, K.V., Solution combustion synthesis of nanoscale materials, *Chem. Rev.*, 2016, vol. 116, no. 23, pp. 14493–14586. doi 10.1021/acs.chemrev.6b00279

29. Rogachev, A.S., Vadchenko, S.G., and Shchukin, A.S., SHS reaction and explosive crystallization in thin films: Resemblance and distinction, *Int. J. Self-Propag. High-Temp. Synth.*, 2017, vol. 26, no. 1, pp. 44–48. doi 10.3103/S1061386217010095

30. Kitchen, H.J., Vallance, S.R., Kennedy, J.L., Tapia-Ruiz, N., Carassiti, L., Harrison, A., Whittaker, A.G., Drysdale, T.D., Kingman, S.W., and Gregory, D.H., Modern microwave methods in solid-state inorganic materials chemistry: From fundamentals to manufacturing, *Chem. Rev.*, 2014, vol. 114, no. 2, pp. 1170–1206. doi 10.1021/cr4002353

31. Merzhanov, A.G., Shkiro, V.M., and Borovinskaya, I.P., A method for synthesis of refractory inorganic compounds, *USSR Inventor's Certificate* 255 221, 1967.

32. Merzhanov, A.G. and Borovinskaya, I.P., Self-propagating high-temperature synthesis of inorganic compounds, *Dokl. Akad. Nauk SSSR*, 1972, vol. 204, no. 2, pp. 366–369.

33. Grigoryan, H., Mukasyan, A., Rogachev, A., and Sytschev, A., International Conference on historical aspects of SHS in different countries dedicated to the 40th anniversary of SHS, *Int. J. Self-Propag. High-Temp. Synth.*, 2007, vol. 16, no. 4, pp. 256–258. doi 10.3103/S1061386207040127

34. Aruna, S.T. and Mukasyan, A.S., Combustion synthesis and nanomaterials, *Curr. Opin. Solid State Mater.*

Sci., 2008, vol. 12, no. 3, pp. 44−50. doi 10.1016/j.cossms.2008.12.002

35. Merzhanov, A.G., The chemistry of self-propagating high-temperature synthesis, *J. Mater. Chem.*, 2004, vol. 14, no. 12, pp. 1779−1786. doi 10.1039/b401358c

36. Specchia, S., Civera, A., Saracco, G., and Specchia, V., Palladium/perovskite/zirconia catalytic premixed fiber burners for efficient and clean natural gas combustion. *Catal. Today*, 2006, vol. 117, no. 4, pp. 427−432. doi 10.1016/j.cattod.2006.06.041

37. Tacchino, S., Vella, L.D., and Specchia, S., Catalytic combustion of CH_4 and H_2 into micro-monoliths, *Catal. Today*, 2010, vol. 157, nos. 1−4, pp. 440−445. doi 10.1016/j.cattod.2010.03.002

38. Specchia, S., Conti, F., and Specchia, V., Kinetic studies on $Pd/Ce_xZr_{1-x}O_2$ catalyst for methane combustion, *Ind. Eng. Chem. Res.*, 2010, vol. 49, no. 21, pp. 11101−11111. doi 10.1021/ie100532x

39. Specchia, S. and Toniato, G., Natural gas combustion catalysts for environmental-friendly domestic burners, *Catal. Today*, 2009, vol. 147S, pp. S99−S106. doi 10.1016/j.cattod.2009.07.033

40. Vita, A., Cristiano, G., Italiano, C., Specchia, S., Cipitì, F., and Specchia, V., Methane oxy-steam reforming reaction: Performances of $Ru/\gamma\text{-}Al_2O_3$ catalysts loaded on structured cordierite monoliths, *Int. J. Hydrogen Energy*, 2014, vol. 39, no. 32, pp. 18592−18603. doi 10.1016/j.ijhydene.2014.03.114

41. Vita, A., Italiano, C., Fabiano, C., Laganà, M., and Pino, L., Influence of Ce-precursor and fuel on structure and catalytic activity of combustion synthesized Ni/CeO_2 catalysts for biogas oxidative steam reforming, *Mater. Chem. Phys.*, 2015, vol. 163, pp. 337−347. doi 10.1016/j.matchemphys.2015.07.048

42. Vita, A., Cristiano, G., Italiano, C., Pino, L., and Specchia, S., Syngas production by methane oxy-steam reforming on Me/CeO_2 (Me = Rh, Pt, Ni) catalyst lined on cordierite monoliths, *Appl. Catal. B: Environ.*, 2015, vol. 162, pp. 551−563. doi 10.1016/j.apcatb.2014.07.028

43. Vita, A., Italiano, C., Fabiano, C., Pino, L., Laganà, M., and Recupero, V., Hydrogen-rich gas production by steam reforming of *n*-dodecane: I. Catalytic activity of Pt/CeO_2 catalysts in optimized bed configuration, *Appl. Catal. B: Environ.*, 2016, vol. 199, pp. 350−360. doi 10.1016/j.apcatb.2016.06.042

44. Italiano, C., Balzarotti, R., Vita, A., Latorrata, S., Fabiano, C., Pino, L., and Cristiani, C., Preparation of structured catalysts with Ni and $Ni\text{−}Rh/CeO_2$ catalytic layers for syngas production by biogas reforming processes, *Catal. Today*, 2016, vol. 273, pp. 3−11. doi 10.1016/j.cattod.2016.01.037

45. Ercolino, G., Stelmachowski, P., and Specchia, S., Catalytic performance of Pd/Co_3O_4 on SiC and ZrO_2 open cell foams for process intensification of methane combustion in lean conditions, *Ind. Eng. Chem. Res.*, 2017, vol. 56, no. 23, pp. 6625−6636. doi 10.1021/acs.iecr.7b01087

46. Ercolino, G., Karimi, S., Stelmachowski, P., and Specchia, S., Catalytic combustion of residual methane on alumina monoliths and open cell foams coated with Pd/Co_3O_4, *Chem. Eng. J.*, 2017, vol. 326, pp. 339−349. doi 10.1016/j.cej.2017.05.149

47. Jain, S.R., Adiga, K.C., and Pai Verneker, V.R., A new approach to thermochemical calculations of condensed fuel-oxidizer mixtures, *Combust. Flame*, 1981, vol. 40, no. C, pp. 71−79. doi 10.1016/0010-2180(81)90111-5

48. Kumar, A., Wolf, E.E., and Mukasyan, A.S., Solution combustion synthesis of metal nanopowders: Nickel-reaction pathways, *AIChE J.*, 2011, vol. 57, no. 8, pp. 2207−2214. doi 10.1002/aic.12416

49. Kumar, A., Wolf, E.E., and Mukasyan, A.S., Solution combustion synthesis of metal nanopowders: Copper and copper/nickel alloys, *AIChE J.*, 2011, vol. 57, no. 12, pp. 3473−3479. doi 10.1002/aic.12537

50. Specchia, S., Ahumada Irribarra, M.A., Palmisano, P., Saracco, G., and Specchia, V., Aging of premixed metal fiber burners for natural gas combustion catalyzed with $Pa/LaMnO_3 \cdot 2ZrO_2$, *Ind. Eng. Chem. Res.*, 2007, vol. 46, no. 21, pp. 6666−6673. doi 10.1021/ie061665y

51. Specchia, S., Finocchio, E., Busca, G., Saracco, G., and Specchia, V., Effect of S-compounds on Pd over $LaMnO_3 \cdot 2ZrO_2$ and $CeO_2 \cdot 2ZrO_2$ catalysts for CH_4 combustion, *Catal. Today*, 2009, vol. 143, nos. 1−2, pp. 86−93. doi 10.1016/j.cattod.2008.10.035

52. Balzarotti, R., Italiano, C., Pino, L., Cristiani, C., and Vita, A., Ni/CeO_2-thin ceramic layer depositions on ceramic monoliths for syngas production by oxy steam reforming of biogas, *Fuel Process. Technol.*, 2016, vol. 149, pp. 40−48. doi 10.1016/j.fuproc.2016.04.002

53. Zavyalova, U., Girgsdies, F., Korup, O., Horn, R., and Schlögl, R., Microwave-assisted self-propagating combustion synthesis for uniform deposition of metal nanoparticles on ceramic monoliths, *J. Phys. Chem. C*, 2009, vol. 113, no. 40, pp. 17493−17501. doi 10.1021/jp905692g

54. Ercolino, G., Stelmachowski, P., Grzybek, G., Kotarba, A., and Specchia, S., Optimization of Pd catalysts supported on Co_3O_4 for low-temperature lean combustion of residual methane, *Appl. Catal. B: Environ.*, 2017, vol. 206, pp. 712−725. doi 10.1016/j.apcatb.2017.01.055

55. Manukyan, K.V., Cross, A., Roslyakov, S., Rouvimov, S., Rogachev, A.S., Wolf, E.E., and Mukasyan, A.S., Solution combustion synthesis of nano-crystalline metallic materials: Mechanistic studies, *J. Phys. Chem. C*, 2013, vol. 117, no. 46, pp. 24417−24427. doi 10.1021/jp408260m

56. Weidenhof, B., Reiser, M., Stöwe, K., Maier, W.F., Kim, M., Azurdia, J., Gulari, E., Seker, E., Barks, A., and Laine, R.M., High-throughput screening of nanoparticle catalysts made by flame spray pyrolysis as hydrocarbon/NO oxidation catalysts, *J. Am. Chem. Soc.*, 2009, vol. 131, no. 26, pp. 9207−9219. doi 10.1021/ja809134s

57. Varma, A. and Lebrat, J.-P., Combustion synthesis of advanced materials, *Chem. Eng. Sci.*, 1992, vol. 47, no. 9, pp. 2179−2194. doi 10.1016/0009-2509(92)87034-N

58. Morsi, K., The diversity of combustion synthesis processing: A review, *J. Mater. Sci.*, 2012, vol. 47, no. 1, pp. 68−92. doi 10.1007/s10853-011-5926-5

59. Moore, J.J. and Feng, H.J., Combustion synthesis of advanced materials: I. Reaction parameters, *Prog. Mater. Sci.*, 1995, vol. 39, no. 4, pp. 243−273. doi 10.1016/0079-6425(94)00011-5

60. Moore, J.J. and Feng, H.J., Combustion synthesis of advanced materials: II. Classification, applications, and modelling, *Prog. Mater. Sci.*, 1995, vol. 39, nos. 4−5, pp. 275−316. doi 10.1016/0079-6425(94)00012-3

61. Erri, P., Pranda, P., and Varma, A., Oxidizer-fuel interactions in aqueous combustion synthesis: I. Iron(III) nitrate model fuels, *Ind. Eng. Chem. Res.*, 2004, vol. 43, no. 12, pp. 3092−3096. doi 10.1021/ie030822f

62. Li, F., Ran, J., Jaroniec, M., Qiao, S.Z., Liang, X.Y., and Ye, Z.Z. Solution combustion synthesis of metal oxide nanomaterials for energy storage and conversion, *Nanoscale*, 2015, vol. 7, no. 42, pp. 17590−17610. doi 10.1039/C5NR05299H

63. Bera, P. and Hegde, M.S., Characterization and catalytic properties of combustion synthesized Au/CeO_2 catalyst, *Catal. Lett.*, 2002, vol. 79, no. 1/4, pp. 75−81. doi 10.1023/A:1015352223861

64. Amjad, U.-E.-S., Vita, A., Galletti, C., Pino, L., and Specchia, S., Comparative study on steam and oxidative steam reforming of methane with noble metal catalysts, *Ind. Eng. Chem. Res.*, 2013, vol. 52, no. 44, pp. 15428−15436. doi 10.1021/ie400679h

65. Farin, B., Monteverde Videla, A.H.A., Specchia, S., and Gaigneaux, E.M., Bismuth molybdates prepared by solution combustion synthesis for the partial oxidation of propene, *Catal. Today*, 2015, vol. 257, no. P1, pp. 11−17. doi 10.1016/j.cattod.2015.03.045

66. Ercolino, G., Grodzka, A., Grzybek, G., Stelmachowski, P., Specchia, S., and Kotarba, A., The effect of the preparation method of Pd-doped cobalt spinel on the catalytic activity in methane oxidation under lean fuel conditions, *Top. Catal.*, 2017, vol. 60, no. 3, pp. 333−341. doi 10.1007/s11244-016-0620-0

67. Toniolo, J.C., Takimi, A.S., and Bergmann, C.P., Nanostructured cobalt oxides (Co_3O_4 and CoO) and metallic Co powders synthesized by solution combustion method, *Mater. Res. Bull.*, 2010, vol. 45, no. 6, pp. 672−676. doi 10.1016/j.materresbull.2010.03.001

68. Sanchez-Dominguez, M., Liotta, L.F., Di Carlo, G., Pantaleo, G., Venezia, A.M., Solans, C., and Boutonnet, M., Synthesis of CeO_2, ZrO_2, $Ce_{0.5}Zr_{0.5}O_2$, and TiO_2 nanoparticles by a novel oil-in-water microemulsion reaction method and their use as catalyst support for CO oxidation, *Catal. Today*, 2010, vol. 158, no. 1, pp. 35−43. doi 10.1016/j.cattod.2010.05.026

69. Liotta, L.F., Di Carlo, G., Pantaleo, G., and Deganello, G., Catalytic performance of Co_3O_4/CeO_2 and $Co_3O_4/CeO_2−ZrO_2$ composite oxides for methane combustion: Influence of catalyst pretreatment temperature and oxygen concentration in the reaction mixture, *Appl. Catal. B: Environ.* 2007, vol. 70, no. 1, pp. 314−322. doi 10.1016/j.apcatb.2005.12.023

70. Kumar, R., Zulfequar, M., Sharma, L., Singh, V.N., and Senguttuvan, T.D., Growth of nanocrystalline $CaCu_3Ti_4O_{12}$ ceramic by the microwave flash combustion method: Structural and impedance spectroscopic studies, *Cryst. Growth Des.*, 2015, vol. 15, no. 3, pp. 1374−1379. doi 10.1021/cg501771k

71. Fino, D., Fino, P., Saracco, G., and Specchia, V., Diesel particulate traps regenerated by catalytic combustion, *Korean J. Chem. Eng.*, 2003, vol. 20, no. 3. pp. 445−450. doi 10.1007/BF02705545

72. Specchia, S., Civera, A., and Saracco, G., In situ combustion synthesis of perovskite catalysts for efficient and clean methane premixed metal burners, *Chem. Eng. Sci.*, 2004, vol. 59, nos. 22−23, pp. 5091−5098. doi 10.1016/j.ces.2004.08.028

73. Specchia, S., Finocchio, E., Busca, G., Palmisano, P., and Specchia, V., Surface chemistry and reactivity of ceria-zirconia-supported palladium oxide catalysts for natural gas combustion, *J. Catal.*, 2009, vol. 263, no. 1, pp. 134−145. doi 10.1016/j.jcat.2009.02.002

74. Morfin, F., Nguyen, T.-S., Rousset, J.-L., and Piccolo, L. Synergy between hydrogen and ceria in Pt-catalyzed CO oxidation: An investigation on $Pt−CeO_2$ catalysts synthesized by solution combustion, *Appl. Catal. B: Environ.*, 2016, vol. 197, pp. 2−13. doi 10.1016/j.apcatb.2016.01.056

75. Purohit, R., Sharma, B., Pillai, K., Tyagi, A. Ultrafine ceria powders via glycine-nitrate combustion, *Mater. Res. Bull.*, 2001, vol. 36, no. 15, pp. 2711−2721. doi 10.1016/S0025-5408(01)00762-0

76. Finocchio, E., Monteverde Videla, A.H.A., and Specchia, S., Surface chemistry and reactivity of $Pd/BaCeO_3·2ZrO_2$ catalyst upon sulphur hydrothermal treatment for the total oxidation of methane, *Appl. Catal. A: Gen.*, 2015, vol. 505, pp. 183−192. doi 10.1016/j.apcata.2015.07.039

77. Piumetti, M., Fino, D., and Russo, N., Mesoporous manganese oxides prepared by solution combustion synthesis as catalysts for the total oxidation of VOCs, *Appl. Catal. B: Environ.*, 2015, vol. 163, pp. 277−287. doi 10.1016/j.apcatb.2014.08.012

78. Berger, D., Matei, C., Voicu, G., and Bobaru, A., Synthesis of $La_{1−x}Sr_xMO_3$ (M = Mn, Fe, Co, Ni) nanopowders by alanine-combustion technique, *J. Eur. Ceram. Soc.*, 2010, 30, no. 2, pp. 617−622. doi 10.1016/j.jeurceramsoc.2009.07.032

79. Ardit, M., Borcănescu, S., Cruciani, G., Dondi, M., Lazău, I., Păcurariu, C., and Zanelli, C., Ni−Ti codoped hibonite ceramic pigments by combustion synthesis: Crystal structure and optical properties, *J. Am. Ceram. Soc.*, 2016, vol. 99, no. 5, pp. 1749−1760. doi 10.1111/jace.14128

80. Vosoughifar, M., Simple route for preparation cobalt tungstate nanoparticles with different amino acids and its photocatalyst application, *J. Mater. Sci. Mater. Electron.*, 2017, vol. 28, no. 11, pp. 8011−8016. doi 10.1007/s10854-017-6505-6

81. Ianoş, R., Lazău, I., Păcurariu, C., and Barvinschi, P., Fuel mixture approach for solution combustion synthesis of $Ca_3Al_2O_6$ powders, *Cem. Concr. Res.*, 2009, vol. 39, no. 7, pp. 566−572. doi 10.1016/j.cemconres.2009.03.014

82. da Silva, A.L.A., Castro, G.G.G., and Souza, M.M.V.M., Synthesis of Sr-doped $LaCrO_3$ powders by combustion method, *J. Therm. Anal. Calorim.*, 2012, vol. 109, no. 1, pp. 33−38. doi 10.1007/s10973-011-1527-4

83. Lazarova, T., Georgieva, M., Tzankov, D., Voykova, D., Aleksandrov, L., Cherkezova-Zheleva, Z., and

Kovacheva, D., Influence of the type of fuel used for the solution combustion synthesis on the structure, morphology and magnetic properties of nanosized $NiFe_2O_4$, *J. Alloys Compd.*, 2017, vol. 700, pp. 272−283. doi 10.1016/j.jallcom.2017.01.055

84. Liu, G., Xin, K., Zhang, L., Wang, B., and He, Y., Glycerol-assisted solution combustion synthesis of improved $LiMn_2O_4$, *Mater. Sci.*, 2013, vol. 31, no. 3, pp. 386−390. doi 10.2478/s13536-013-0115-7

85. Zavyalova, U., Scholz, P., and Ondruschka, B., Influence of cobalt precursor and fuels on the performance of combustion synthesized $Co_3O_4/\gamma\text{-}Al_2O_3$ catalysts for total oxidation of methane, *Appl. Catal. A: Gen.*, 2007, vol. 323, pp. 226−233. doi 10.1016/j.apcata.2007.02.021

86. Zavyalova, U., Nigrovski, B., Pollok, K., Langenhorst, F., Müller, B., Scholz, P., and Ondruschka, B., Gel-combustion synthesis of nanocrystalline spinel catalysts for VOCs elimination, *Appl. Catal. B: Environ.*, 2008, vol. 83, no. 3, pp. 221−228. doi 10.1016/j.apcatb.2008.02.015

87. Pino, L., Vita, A., Cipitì, F., Laganà, M., and Recupero, V., Performance of Pt/CeO_2 catalyst for propane oxidative steam reforming, *Appl. Catal. A: Gen.*, 2006, vol. 306, pp. 68−77. doi 10.1016/j.apcata.2006.03.031

88. Renuka, L., Anantharaju, K.S., Vidya, Y.S., Nagaswarupa, H.P., Prashantha, S.C., Sharma, S.C., Nagabhushana, H., and Darshan, G.P., A simple combustion method for the synthesis of multi-functional ZrO_2/CuO nanocomposites: Excellent performance as sunlight photocatalysts and enhanced latent fingerprint detection, *Appl. Catal. B: Environ.*, 2017, vol. 210, pp. 97−115. doi 10.1016/j.apcatb.2017.03.055

89. Cipitì, F., Barbera, O., Briguglio, N., Giacoppo, G., Italiano, C., and Vita, A., Design of a biogas steam reforming reactor: A modelling and experimental approach, *Int. J. Hydrogen Energy*, 2016, vol. 41, no. 27, pp. 11577−11583. doi 10.1016/j.ijhydene.2015.12.053

90. Barbato, P.S., Colussi, S., Di Benedetto, A., Landi, G., Lisi, L., Llorca, J., and Trovarelli, A, Origin of high activity and selectivity of CuO/CeO_2 catalysts prepared by solution combustion synthesis in CO-PROX reaction, *J. Phys. Chem. C*, 2016, vol. 120, no. 24, pp. 13039−13048. doi 10.1021/acs.jpcc.6b02433

91. Bera, P., Malwadkar, S., Gayen, A., Satyanarayana, C.V.V., Rao, B.S., and Hegde, M.S., Low-temperature water gas shift reaction on combustion synthesized $Ce_{1-x}Pt_xO_{2-\delta}$ catalyst, *Catal. Lett.*, 2004, vol. 96, nos. 3−4, pp. 213−219. doi 10.1023/B:CATL.0000030123.41351.14

92. Tummino, M.L., Laurenti, E., Deganello, F., Bianco Prevot, A., and Magnacca, G., Revisiting the catalytic activity of a doped $SrFeO_3$ for water pollutants removal: Effect of light and temperature, *Appl. Catal. B: Environ.*, 2017, vol. 207, pp. 174−181. doi 10.1016/j.apcatb.2017.02.007

93. Deganello, F., Marcì, G., and Deganello, G., Citrate−nitrate auto-combustion synthesis of perovskite-type nanopowders: A systematic approach, *J. Eur. Ceram. Soc.*, 2009, 29, no. 3, pp. 439−450. doi 10.1016/j.jeurceramsoc.2008.06.012

94. Yilmaz, E., Sonmez, M.S., Derin, B., Sahin, F.C., and Yucel, O., Synthesis of Mn_2O_3 nanopowders with urea and citric acid by solution combustion route, in *Proc. 146th Ann. TMS Meeting and Exhibition*, 2017, pp. 39−46. doi 10.1007/978-3-319-51493-2_510.1007/978-3-319-51493-2_5

95. Marinšek, M., Zupan, K., and Maèek, J., Ni−YSZ cermet anodes prepared by citrate/nitrate combustion synthesis, *J. Power Sources*, 2002, vol. 106, no. 1, pp. 178−188. doi 10.1016/S0378-7753(01)01056-4

96. Kolb, G., Baier, T., Schürer, J., Tiemann, D., Ziogas, A., Specchia, S., Galletti, C., Germani, G., and Schuurman, Y., A micro-structured 5 kW complete fuel processor for iso-octane as hydrogen supply system for mobile auxiliary power units: II. Development of water-gas shift and preferential oxidation catalysts reactors and assembly of the fuel processor, *Chem. Eng. J.*, 2008, vol. 138, nos. 1−3, pp. 474−489. doi 10.1016/j.cej.2007.06.037

97. Shi, L., Tao, K., Kawabata, T., Shimamura, T., Zhang, X.J., and Tsubaki, N., Surface impregnation combustion method to prepare nanostructured metallic catalysts without further reduction: As-burnt Co/SiO_2 catalysts for Fischer−Tropsch synthesis, *ACS Catal.*, 2011, vol. 1, pp. 1225−1233. doi 10.1021/cs200294d

98. Xanthopoulou, G. and Vekinis, G., Deep oxidation of methane using catalysts and carriers produced by self-propagating high-temperature synthesis, *Appl. Catal. A: Gen.*, 2000, vol. 199, no. 2, pp. 227−238. doi 10.1016/S0926-860X(99)00562-1

99. Anuradha, T., Ranganathan, S., Mimani, T., and Patil, K., Combustion synthesis of nanostructured barium titanate, *Scr. Mater.*, 2001, vol. 44, nos. 8−9, pp. 2237−2241. doi 10.1016/S1359-6462(01)00755-2

100. Deshpande, K., Mukasyan, A., and Varma, A., Direct synthesis of iron oxide nanopowders by the combustion approach: Reaction mechanism and properties, *Chem. Mater.*, 2004, vol. 16, no. 24, pp. 4896−4904. doi 10.1021/CM040061M

101. Manoharan, S.S., Swati Prasanna, S.J., Rao, M.L., and Sahu, R.K., Microwave-assisted synthesis of fine particle oxides employing wet redox mixtures, *J. Am. Ceram. Soc.*, 2002, vol. 85, no. 10, pp. 2469−2471. doi 10.1111/j.1151-2916.2002.tb00482.x

102. Jardim, E.O., Rico-Francés, S., Coloma, F., Anderson, J.A., Silvestre-Albero, J., and Sepúlveda-Escribano, A., Influence of the metal precursor on the catalytic behavior of Pt/Ceria catalysts in the preferential oxidation of CO in the presence of H_2 (PROX), *J. Colloid Interface Sci.*, 2015, vol. 443, pp. 45−55. doi 10.1016/j.jcis.2014.12.013

103. Santos, A.C.S.F., Damyanova, S., Teixeira, G.N.R., Mattos, L.V., Noronha, F.B., Passos, F.B., and Bueno, J.M.C., The effect of ceria content on the performance of $Pt/CeO_2/Al_2O_3$ catalysts in the partial oxidation of methane, *Appl. Catal. A: Gen.*, 2005, vol. 290, no. 1, pp. 123−132. doi 10.1016/j.apcata.2005.05.015

104. Kumar, A., Mukasyan, A.S., and Wolf, E.E., Combustion synthesis of Ni, Fe, and Cu multi-component catalysts for hydrogen production from ethanol reforming, *Appl. Catal. A: Gen.*, 2011, vol. 401, no. 1, pp. 20−28. doi 10.1016/j.apcata.2011.04.038

105. Galletti, C., Specchia, S., Saracco, G., and Specchia, V., CO preferential oxidation in H_2-rich gas for fuel cell applications: Microchannel reactor performance with Rh-based catalyst, *Int. J. Hydrogen Energy*, 2008, vol. 33, no. 12, pp. 3045–3048. doi 10.1016/j.ijhydene.2008.01.032

106. Vita, A., Ashraf, M.A., Italiano, C., Fabiano, C., and Specchia, S., Syngas production by biogas steam and oxy steam reforming processes on Rh/CeO_2 catalyst coated on ceramics monolith and open foams, in *AIChE Proceedings*, 2015, no. 402e. https://aiche.confex.com/aiche/2015/webprogram/Paper427656.html. Accessed May 30, 2017.

107. Cross, A., Kumar, A., Wolf, E.E., and Mukasyan, A.S., Combustion synthesis of a nickel supported catalyst: Effect of metal distribution on the activity during ethanol decomposition, *Ind. Eng. Chem. Res.*, 2012, vol. 51, no. 37, pp. 12004–12008. doi 10.1021/ie301478n

108. Deshpande, K., Mukasyan, A.S., and Varma, A., High throughput evaluation of perovskite-based anode catalysts for direct methanol fuel cells, *J. Power Sources*, 2006, vol. 158, no. 1, pp. 60–68. doi 10.1016/j.jpowsour.2005.09.025

109. Wen, W., Wu, J.-M., and Cao, M.-H., Rapid one-step synthesis and electrochemical performance of NiO/Ni with tunable macroporous architectures, *Nano Energy*, 2013, vol. 2, no. 6, pp. 1383–1390. doi 10.1016/j.nanoen.2013.07.002

110. Raza, M.A., Rahman, I.Z., and Beloshapkin, S., Synthesis of nanoparticles of $La_{0.75}Sr_{0.25}Cr_{0.5}Mn_{0.5}O_{3-\delta}$ (LSCM) perovskite by solution combustion method for solid oxide fuel cell application, *J. Alloys Compd.*, 2009, vol. 485, no. 1, pp. 593–597. doi 10.1016/j.jallcom.2009.06.059

111. Li, X., Xiao, Q., Liu, B., Lin, H., and Zhao, J., One-step solution-combustion synthesis of complex spinel titanate flake particles with enhanced lithium-storage properties, *J. Power Sources*, 2015, vol. 273, pp. 128–135. doi 10.1016/j.jpowsour.2014.08.129

112. Roy, B., Martinez, U., Loganathan, K., Datye, A.K., and Leclerc, C.A., Effect of preparation methods on the performance of Ni/Al_2O_3 catalysts for aqueous-phase reforming of ethanol: I. Catalytic activity, *Int. J. Hydrogen Energy*, 2012, vol. 37, no. 10, pp. 8143–8153. doi 10.1016/j.ijhydene.2012.02.056

113. Roy, B., Artyushkova, K., Pham, H.N., Li, L., Datye, A.K., and Leclerc, C.A., Effect of preparation method on the performance of the Ni/Al_2O_3 catalysts for aqueous-phase reforming of ethanol: II. Characterization, *Int. J. Hydrogen Energy*, 2012, vol. 37, no. 24, pp. 18815–18826. doi 10.1016/j.ijhydene.2012.09.098

114. Monteverde Videla, A.H.A., Stelmachowski, P., Ercolino, G., and Specchia, S., Benchmark comparison of Co_3O_4 spinel structured oxides with different morphologies for oxygen evolution reaction under alkaline conditions, *J. Appl. Electrochem.*, 2017, vol. 47, no. 3, pp. 295–304. doi 10.1007/s10800-016-1040-3

115. Aliotta, C., Liotta, L.F., Deganello, F., Parola, V., and La Martorana, A., Direct methane oxidation on $La_{1-x}Sr_xCr_{1-y}Fe_yO_{3-\delta}$ perovskite-type oxides as potential anode for intermediate temperature solid oxide fuel cells, *Appl. Catal. B: Environ.*, 2016, vol. 180, pp. 424–433. doi 10.1016/j.apcatb.2015.06.012

116. Bharathidasan, T., Mandalam, A., Balasubramanian, M., Dhandapani, P., Sathiyanarayanan, S., and Mayavan, S., Zinc oxide-containing porous boron–carbon–nitrogen sheets from glycine–nitrate combustion: Synthesis, self-cleaning, and sunlight-driven photocatalytic activity, *ACS Appl. Mater. Interf.*, 2015, vol. 7, no. 33, pp. 18450–18459. doi 10.1021/acsami.5b04609

117. Bera, P., Patil, K.C., Jayaram, V., Subbanna, G.N., and Hegde, M.S., Ionic dispersion of Pt and Pd on CeO_2 by combustion method: Effect of metal–ceria interaction on catalytic activities for NO reduction and CO and hydrocarbon oxidation, *J. Catal.*, 2000, vol. 196, no. 2, pp. 293–301. doi 10.1006/jcat.2000.3048

118. Saracco, G., Badini, C., and Specchia, V., Catalytic traps for diesel particulate control, *Chem. Eng. Sci.*, 1999, vol. 54, nos. 15–16, pp. 3035–3041. doi 10.1016/S0009-2509(98)00462-X

119. Saracco, G. and Specchia, V., Simultaneous removal of nitrogen oxides and fly-ash from coal-based power-plant flue gases, *Appl. Therm. Eng.*, 1998, vol. 18, no. 11, pp. 1025–1035. doi 10.1016/S1359-4311(98)00035-0

120. Saracco, G., Specchia, S., and Specchia, V., Catalytically modified fly-ash filters for NO_x reduction with NH_3, *Chem. Eng. Sci.*, 1996, vol. 51, no. 24, pp. 5289–5297. doi 10.1016/S0009-2509(96)00373-9

121. Bera, P., Aruna, S.T., Patil, K.C., and Hegde, M.S., Studies on Cu/CeO_2: A new NO reduction catalyst, *J. Catal.*, 1999, vol. 186, no. 1, pp. 36–44. doi 10.1006/jcat.1999.2532

122. Granger, P. and Parvulescu, V.I., Catalytic NO_x abatement systems for mobile sources: From three-way to lean burn after-treatment technologies, *Chem. Rev.*, 2011, vol. 111, no. 5, pp. 3155–3207. doi 10.1021/cr100168g

123. Galletti, C., Djinović, P., Specchia, S., Batista, J., Levec, J., Pintar, A., and Specchia, V., Influence of the preparation method on the performance of Rh catalysts on CeO_2 for WGS reaction, *Catal. Today*, 2011, vol. 176, no. 1, pp. 336–339. doi 10.1016/j.cattod.2010.11.069

124. Nguyen, T.-S., Morfin, F., Aouine, M., Bosselet, F., Rousset, J.L., and Piccolo, L., Trends in the CO oxidation and PROX performances of the platinum-group metals supported on ceria, *Catal. Today*, 2015, vol. 253, pp. 106–114. doi 10.1016/j.cattod.2014.12.038

125. Stelmachowski, P., Kopacz, A., Legutko, P., Indyka, P., Wojtasik, M., Ziemiański, L., Zak, G., Sojka, Z., and Kotarba, A., The role of crystallite size of iron oxide catalyst for soot combustion, *Catal. Today*, 2015, vol. 257, no. P1, pp. 111–116. doi 10.1016/j.cattod.2015.02.018

126. Specchia, S., Tacchino, S., and Specchia, V., Facing the catalytic combustion of CH_4/H_2 mixtures into monoliths, *Chem. Eng. J.*, 2011, vol. 167, nos. 2–3, pp. 622–633. doi 10.1016/j.cej.2010.10.051

127. Ugues, D., Specchia, S., and Saracco, G., Optimal microstructural design of a catalytic premixed FeCrAlloy fiber burner for methane combustion, *Ind.*

Eng. Chem. Res., 2004, vol. 43, no. 9, pp. 1990−1998. doi 10.1021/ie034202q

128. Ziaei-Azad, H., Khodadadi, A., Esmaeilnejad-Ahranjani, P., and Mortazavi, Y., Effects of Pd on enhancement of oxidation activity of LaBO$_3$ (B = Mn, Fe, Co, and Ni) pervoskite catalysts for pollution abatement from natural gas fueled vehicles, *Appl. Catal. B: Environ.*, 2011, vol. 102, nos. 1−2, pp. 62−70. doi 10.1016/j.apcatb.2010.11.025

129. du Plessis, J.P. and Woudberg, S., Pore-scale derivation of the Ergun equation to enhance its adaptability and generalization, *Chem. Eng. Sci.*, 2008, vol. 63, no. 9, pp. 2576−2586. doi 10.1016/j.ces.2008.02.017

130. Tzimpilis, E., Moschoudis, N., Stoukides, M., and Bekiaroglou, P., Preparation, active phase composition, and Pd content of perovskite-type oxides, *Appl. Catal. B: Environ.*, 2008, vol. 84, no. 3, pp. 607−615. doi 10.1016/j.apcatb.2008.05.016

131. Cristiani, C., Visconti, C.G., Finocchio, E., Gallo Stampino, P., and Forzatti, P., Towards the rationalization of the washcoating process conditions, *Catal. Today*, 2009, vol. 147S, pp. S24−S29. doi 10.1016/j.cattod.2009.07.031

132. Almeida, L.C., Echave, F.J., Sanz, O., Centeno, M.A., Odriozola, J.A., and Montes, M., Washcoating of metallic monoliths and microchannel reactors, *Stud. Surf. Sci. Catal.*, 2010, vol. 175, pp. 25−33. doi 10.1016/S0167-2991(10)75004-7

133. IEA−WEO-2016. http://www.worldenergyoutlook.org/publications/weo-2016/. Accessed May 3, 2017.

134. The Paris Agreement. http://unfccc.int/paris_agreement/items/9485.php. Accessed May 3, 2017.

135. Reay, D.A., Ramshaw, C., and Harvey, A.P., *Process Intensification: Engineering for Efficiency, Sustainability, and Flexibility*, Amsterdam: Elsevier−Butterworth−Heinemann, 2008.

136. Stankiewicz, A.I. and Moulijn, J.A., Process intensification: Transforming chemical engineering, *Chem. Eng. Prog.*, 2000, vol. 96, pp. 22−34.

137. van Gerven, T. and Stankiewicz, A., Structure, energy, synergy, time-the fundamentals of process intensification, *Ind. Eng. Chem. Res.*, 2009, vol. 48, no. 5, pp. 2465−2474. doi 10.1021/ie801501y

138. Avila, P., Montes, M., and Miró, E.E., Monolithic reactors for environmental applications: A review on preparation technologies, *Chem. Eng. J.*, 2005, vol. 109, no. 1, pp. 11−36. doi 10.1016/j.cej.2005.02.025

139. Twigg, M.V. and Richardson, J.T., Fundamentals and applications of structured ceramic foam catalysts, *Ind. Eng. Chem. Res.*, 2007, vol. 46, no. 12, pp. 4166−4177. doi 10.1021/ie061122o

140. Buciuman, F.C. and Kraushaar-Czarnetzki, B., Ceramic foam monoliths as catalyst carriers: I. Adjust-

ment and description of the morphology, *Ind. Eng. Chem. Res.*, 2003, vol. 42, no. 9, pp. 1863−1869. doi 10.1021/ie0204134

141. Huo, W.-L., Zhang, X.-Y., Chen, Y.-G., Lu, Y.-J., Liu, W.-T., Xi, X.-Q., Wang, Y.-L., Xu, J., and Yang, J.-L., Highly porous zirconia ceramic foams with low thermal conductivity from particle-stabilized foams, *J. Am. Ceram. Soc.*, 2016, vol. 99, no. 11, pp. 3512−3515. doi 10.1111/jace.14555

142. Bianchi, E., Heidig, T., Visconti, C.G., Groppi, G., Freund, H., and Tronconi, E., An appraisal of the heat transfer properties of metallic open-cell foams for strongly exo-/endo-thermic catalytic processes in tubular reactors, *Chem. Eng. J.*, vol. 198−199, pp. 512−528. doi 10.1016/j.cej.2012.05.045

143. Richardson, J.T., Peng, Y., and Remue, D., Properties of ceramic foam catalyst supports: Pressure drop, *Appl. Catal. A: Gen.*, 2000, vol. 204, no. 1, pp. 19−32. doi 10.1016/S0926-860X(00)00508-1

144. Richardson, J.T., Remue, D., and Hung, J.K., Properties of ceramic foam catalyst supports: Mass and heat transfer, *Appl. Catal. A: Gen.*, vol. 250, no. 2, pp. 319−329. doi 10.1016/S0926-860X(03)00287-4

145. Tronconi, E., Groppi, G., and Visconti, C.G., Structured catalysts for non-adiabatic applications, *Curr. Opin. Chem. Eng.*, 2014, vol. 5, pp. 55−67. doi 10.1016/j.coche.2014.04.003

146. Tappan, B.C., Huynh, M.H., Hiskey, M.A., Chavez, D.E., Luther, E.P., Mang, J.T., and Son, S.F., Ultralow-density nanostructured metal foams: Combustion synthesis, morphology, and composition, *J. Am. Chem. Soc.*, 2006, vol. 128, no. 20, pp. 6589−6594. doi 10.1021/ja056550k

147. Specchia, S., Fuel processing activities at European level: A panoramic overview, *Int. J. Hydrogen Energy*, 2014, vol. 39, no. 21, pp. 17953−17968. doi 10.1016/j.ijhydene.2014.04.040

148. Carmo, M., Fritz, D.L., Mergel, J., and Stolten, D., A comprehensive review on PEM water electrolysis, *Int. J. Hydrogen Energy*, 2013, vol. 38, no. 12, pp. 4901−4934. doi 10.1016/j.ijhydene.2013.01.151

149. Xuan, J., Leung, M.K.H., Leung, D.Y.C., and Ni, M., A review of biomass-derived fuel processors for fuel cell systems, *Renew. Sustain. Energy Rev.*, 2009, vol. 13, no. 6, pp. 1301−1313. doi 10.1016/j.rser.2008.09.027

150. Shen, Y., Linville, J.L., Urgun-Demirtas, M., Mintz, M.M., and Snyder, S.W., An overview of biogas production and utilization at full-scale wastewater treatment plants (WWTPs) in the United States: Challenges and opportunities towards energy-neutral WWTPs, *Renew. Sustain. Energy Rev.*, 2015, vol. 50, pp. 346−362. doi 10.1016/j.rser.2015.04.129